# SOIL BEHAVIOR TYPE CLASSIFICATION SYSTEM BASED ON CONE PENETRATION TEST

**Peter K. Robertson**
*Technical Advisor, Gregg Drilling & Testing Inc., California, USA*

## ABSTRACT

A soil classification system is used to group soils according to shared qualities or characteristics based on simple cost effective tests. The most common soil classification systems used in geotechnical engineering are based on physical (textural) characteristics such as grain size and plasticity. Ideally, geotechnical engineers would also like to classify soils based on behavior characteristics that have a strong link to fundamental in-situ behavior. Existing textural-based classification systems have a weak link to in-situ behavior since they are measured on disturbed and remolded samples. The cone penetration test (CPT) has been gaining in popularity for site investigations due to the cost effective, rapid, continuous and reliable measurements. The most common CPT-based classification systems are based on behavior characteristics and are often referred to as a Soil Behavior Type (SBT) classification. This paper presents an update of popular CPT-based SBT classification systems to use behavior-based descriptions. The update includes a method to identify the existence of microstructure in soils and examples are used to illustrate the advantages and limitations of such a system.

## 1 INTRODUCTION

This paper is a shorter version of a paper in the Canadian Geotechnical Journal (Robertson, 2016). A soil classification system is used to group soils according to shared qualities or characteristics based on simple cost effective tests. The most common soil classification systems used in geotechnical engineering are based on physical (textural) characteristics such as grain size and plasticity (e.g. Unified Soil Classification System). These textural-based classification systems have been used for over 70 years to provide general guidance through empirical correlations based on past field experience. Unfortunately, empirical correlations between simple physical index properties measured on remolded samples and in-situ soil behavior have significant uncertainty. Ideally, geotechnical engineers should also classify soils based on fundamental behavior characteristics that have a strong link to in-situ behavior. A combined classification based on both physical and behavior characteristics would be very helpful for many geotechnical projects.

The cone penetration test (CPT) has been gaining in popularity for site investigations due to the cost effective, rapid, continuous and reliable measurements. The most common CPT-based classification systems are based on behavior characteristics and are often referred to as a Soil Behavior Type (SBT) classification (e.g. Robertson, 1990). However, most CPT-based SBT classification systems use textural-based descriptions, such as sand and clay that can cause some confusion in geotechnical practice. The objective of this paper is to present an update to the Robertson (1990, 2009) and Schneider et al (2008) CPT-based SBT classification system with behavior-based descriptions for each soil group. The importance of microstructure and how it can influence CPT-based classification is also discussed. The paper will also collate, update and summarize the growing experience that exists to guide in the classification of soils based on CPT measurements.

## 2 SOIL CLASSIFICATION

The most common soil classification system used by engineers and geologists in North America is the Unified Soil Classification System, USCS (ASTM D 2487-11). The system, similar to others used around the world, is based on physical characteristics of grain-size distribution and plasticity (Atterberg Limits) measured on disturbed and remolded samples. The USCS groups soils into two broad groups: coarse-grained (sand and gravel) and fine-grained (silt and clay). Coarse-grained soils are those with more than 50% retained on or above the #200 sieve (>0.075mm) and are further grouped based on grain size and fines content (e.g. silty sand). Fine-grained soils are those with 50% or more passing the #200 sieve and are further grouped based on plasticity (high or low).

The actual in-situ soil behavior depends on many other factors such as geologic processes related to origin, environmental factors (such as stress history) as well as physical and chemical processes. In general, soils tend to become stiffer and stronger with age. The successful link between simple physical characteristics and in-situ behavior is strongly influenced by geologic factors such as age and cementation. Typically, the link is most successful when applied to young (Holocene and Pleistocene-age), uncemented silica-based deposits with limited stress and strain history (e.g. older heavily overconsolidated clays can have similar strength and compressibility characteristics to younger uncemented sands).

# 3 GENERALIZED SOIL BEHAVIOR

The behavior of natural soils is complex with many extensive publications attempting to describe this behavior (e.g. Leroueil and Hight, 2003). The following is a very short summary of some key features of soil behavior as it relates to a possible behavior type classification system.

The following features describe the essential elements of soil behavior (e.g. Atkinson, 2007):

- Soil can change in volume due to rearrangement of grains and void space changes.
- Soil is essentially frictional where strength and stiffness increases with normal stress and with depth in the ground.
- Soil is essentially inelastic where response is non-linear to loading beyond an initial very small threshold strain.

As stated above, in-situ soil behavior depends on many factors such as geologic processes related to origin (e.g. depositional and compositional features), environmental factors (e.g. stress and temperature), as well as physical and chemical processes (e.g. aging and cementation). The powerful early concepts of Critical State Soil Mechanics (CSSM) were based on tests performed on isotropically consolidated reconstituted (clay) samples and can be representative of saturated '*ideal soils'* (Leroueil and Hight, 2003). Many natural soils have some form of structure that can make the in-situ behavior different from those of '*ideal soils'*. The term structure can be used to describe features either at the deposit scale (macrostructure), e.g. layering and fissures, or at the particle scale (microstructure), e.g. bonding/cementation. Older natural soils tend to have some microstructure caused by post depositional factors, of which the primary ones tend to be age and bonding (cementation).

Many authors have discussed the effects of microstructure (e.g. Burland, 1990, Leroueil, 1992, Leroueil and Hight, 2003). Microstructure can be caused by many factors such as: secondary compression, thixotropy, cementation, cold welding, and aging (Leroueil and Hight, 2003). Microstructure tends to give a soil a strength and stiffness that cannot be accounted for by void ratio and stress history alone. Compared to the same '*ideal soil*' at the same void ratio, the *'structured soil'* with microstructure has higher yield stress, peak strength and small strain stiffness. At larger strains, when the effects of microstructure can be destroyed due to factors such as; compression, shearing, swelling, weathering and fatigue, the soil becomes '*destructured*' (Leroueil and Hight, 2003). The term *'ideal soil'* will be used to describe soils with little or no microstructure that are predominately young and uncemented. The term *'structured soil'* will be used to describe soils with extensive microstructure, such as caused by aging and cementation.

CSSM is based on the observation that soils ultimately reach critical state (CS) at large strains and at critical state there is a unique relationship between shear stress, normal effective stress and void ratio. Since critical state is independent of the initial state, the parameters that define critical state depend only on the nature of the grains of the soils and can be linked to basic soil classification (e.g. Atkinson, 2007). The current in-situ state of a soil can be defined in a number of ways. In fine-grained soil, it is common to define the current state in terms of overconsolidation ratio (OCR) that is related to the normal compression line (NCL), since fine-grained '*ideal soils'* tend to have a unique NCL that is essentially parallel to the CSL. In coarse-grained soil, it is still common to define in-situ state in terms of relative density (or density index), especially for clean sands. However, it is becoming more common to define the current state in terms of a state parameter ($\psi$) that is related to the CSL, since the NCL is not unique (e.g. Been and Jefferies, 1985). At low confining stress the CSL for many clean silica-based sands can be very flat in terms of void ratio versus log mean effective stress and hence, there is an approximate link between relative density and state parameter. However, state parameter can capture the current state for most coarse-grained soils over a wide range of stress.

There is an important difference between the behavior of '*ideal soils'* that are either 'loose' or 'dense' of CS. Soils that are 'loose' of CS tend to contract on drained loading (or where pore pressures rise on undrained shear). Soils that are 'dense' of CS tend to dilate at large shear strains (or where pore pressures can decrease in undrained loading). The tendency of soils to change volume while shearing is called dilatancy and is a fundamental aspect of soil behavior.

The behavior of soil in shear prior to failure can be classified into two groups; soils that dilate at large strains and soils that contract at large strains. Saturated soils that contract at large strains have a shear strength in undrained loading that is lower than the strength in drained loading, whereas saturated soils that dilate at large strains tend to have a shear strength in undrained loading that is either equal to or larger than in drained loading. When saturated soils contract at large strain, they may also show a strain softening response in undrained shearing, although not all soils that contract show a strain softening response in undrained shear. This strength loss in undrained shear can result in instability given an appropriate geometry, such as flow liquefaction (e.g. Robertson, 2010). Hence, classification of soils that are either contractive or dilative at large strains can be an important behavior characteristic for many geotechnical problems.

Jefferies and Been (2006) had suggested that coarse-grained *'ideal soils'* with a state parameter $\psi < -0.05$ will tend to dilate at large strains when loaded in drained shear. Hence, coarse-grained saturated *'ideal soils'* with $\psi < -0.05$ will tend to generate a decrease in pore pressure and an increase in effective stress at larger strains in undrained shear and tend to be strain hardening. Likewise, fine-grained saturated '*ideal soils'* with an OCR > 4 tend to dilate when loaded in drained shear and also tend to generate a decrease in pore pressure in undrained shear. Most soils tend to contract at small strains (i.e. develop positive pore pressures under undrained loading), which is a major feature in soils that experience cyclic liquefaction. Clearly classifying soils by their tendency to dilate or contract at large strains under shearing is an important behavior characteristic since it can guide the engineer in terms of appropriate behavior parameters and critical loading conditions.

Idriss and Boulanger (2008) classified soils as either sand-like or clay-like in their behavior, where sand-like soils are susceptible to cyclic liquefaction and clay-like soils are not susceptible to cyclic liquefaction. Idriss and Boulanger (2008) also suggested that fine-grained soils transition from behavior that is more fundamentally like sands to behavior that is more fundamentally like clays over a fairly narrow range of plasticity index (PI). Sand-like soils tend to have PI < 10% and clay-like soils tend to have PI > 18% (Bray and Sancio, 2006). The transition from more sand-like to more clay-like behavior is conceptually similar to the transition in the USCS from coarse-grained (non-plastic) to fine-grained (plastic) soils, although some low or non-plastic fine-grained soils (e.g. ML and CL) can behave more sand-like, as suggested by Idriss and Boulanger (2008). Likewise, the transition from saturated soils that are more sand-like to more clay-like typically corresponds to a response that transitions from one that is predominately drained under most static loading to a response that is predominately undrained under most static loading, although the rate of loading also has a major role.

A modified classification system based on behavior characteristics can be built around groupings that divide soils that show either dilative or contractive behavior at large strains and soils that are predominately more sand-like or more clay-like. There can also be a group that captures soils that are in transition from more sand-like to more clay-like, since the change occurs over a range of behavior type.

Since natural soil behavior is complex, any classification system based on behavior characteristics should involve multiple measurements that are repeatable and capture different aspects of in-situ soil behavior. For classification systems to be effective and easy to use they must also be based on rather simple, cost effective repeatable tests. For an in-situ test to meet these demands, the test should be simple, cost effective and provide several repeatable independent measurements. One of the most popular modern in-situ test that is applicable to most uncemented soil is the cone penetration test (CPT). The CPT is fast (20mm/s), cost effective and provides continuous and repeatable measurements of several parameters. The basic CPT records tip resistance ($q_c$) and sleeve resistance ($f_s$). The CPTu provides the addition of penetration pore pressure (u), often in the $u_2$ location just behind the tip, combined with a measure of the rate of pore pressure dissipation during a pause in the penetration process, often expressed as the time required to dissipate 50% of the excess pore pressure ($t_{50}$). The CPTu can also provide in-situ equilibrium pore pressure after 100% dissipation ($u_o$) that is helpful

to define the in-situ piezometric profile at the time of the CPTu. The seismic CPTu (SCPTu) provides the additional measurement of in-situ shear wave velocity ($V_s$) and, in some conditions, in-situ compression wave velocity ($V_p$). Hence, the SCPTu can provide up to 7 independent measurements in one cost effective test. Ideally a classification system should include all these measurements to be fully effective. However, a practical classification system can still be effective based on either 2 or 3 measurements, provided limits are placed on the range of applicable soils (e.g. restricted to predominately '*ideal soils'*).

Any behavior based classification systems will tend to apply primarily to '*ideal soils'* that have little or no microstructure. Hence, it can be important to have a system and associated in-situ test that can also provide a method to identify if the soil to be classified has a behavior similar to most '*ideal soils'*, i.e. has little or no microstructure. It will be shown that the SCPTu measurements have the potential to identify soils with significant microstructure.

# 4 EXISTING CPT-BASED CLASSIFICATION

One of the major applications of the CPT has been the determination of soil stratigraphy and the identification of soil type. This has been accomplished using charts that link cone measurements to soil type. The early charts developed in the Netherlands were based on measured cone resistance, $q_c$ and sleeve resistance, $f_s$ using a mechanical cone (e.g. Begemann, 1965) and showed that there is an approximate linear link between $q_c$ and $f_s$ for a given soil type. Early charts using $q_c$ and friction ratio ($R_f = f_s/q_c$ in percent) where proposed by Douglas and Olsen (1981), but the charts proposed by Robertson et al. (1986) and Robertson (1990, 2009) have become very popular. Robertson et al (1986) and Robertson (1990, 2009) stressed that the charts were predictive of Soil Behavior Type (SBT), since the cone responds to the in-situ mechanical behavior of the soil (e.g. strength, stiffness, compressibility and drainage) and not directly to classification criteria based on physical characteristics, such as grain-size distribution and soil plasticity.

The CPT-based normalized Soil Behavior Type (SBTn) method suggested by Robertson (1990) was based on the following normalized parameters:

$$Q_{t1} = (q_t - \sigma_{vo})/\sigma'_{vo} \quad (1)$$

$$F_r = [(f_s/(q_t - \sigma_{vo})] \, 100\% \quad (2)$$

$$B_q = (u_2 - u_0) / (q_t - \sigma_{vo}) = \Delta u / (q_t - \sigma_{vo}) \quad (3)$$

where:
$q_t$ = cone resistance corrected for water effects, where $q_t = q_c + u_2(1\text{-}a)$
a = cone area ratio, typically around 0.8
$\sigma_{vo}$ = current in-situ total vertical stress
$\sigma'_{vo}$ = current in-situ effective vertical stress
$u_2$ = penetration pore pressure (immediately behind cone tip)
$u_0$ = current in-situ equilibrium water pressure
$\Delta u$ = excess penetration pore pressure = $(u_2 - u_o)$

Robertson (1990) suggested two charts based on either $Q_{t1}$ - $F_r$ and $Q_{t1}$ - $B_q$ but recommended that the $Q_{t1}$ - $F_r$ chart (illustrated in Figure 1) was generally more reliable, since the CPT penetration pore pressures ($u_2$) can suffer from lack of repeatability due to loss of saturation, especially when performed onshore at locations where the water table is deep and/or in very stiff soils. The sleeve resistance ($f_s$) is often considered less reliable than the cone resistance ($q_c$) due to variations in cone design (e.g. Lunne et al, 1986). However, Boggess and Robertson (2010) provided recommendations on methods to improve the repeatability and reliability of sleeve resistance measurements by using cone designs with separate load cells, equal end areas sleeves, attention to tolerance requirements and careful test procedures. Robertson (2009) also showed that, in softer soils, the SBTn charts are not overly sensitive to variations in $f_s$. The chart shown in Figure 1 is based on the corrected cone resistance ($q_t$) that requires pore pressure measurements to make the correction. However, the difference between $q_c$ and $q_t$ is generally small, except in very soft fine-grained soils. Hence, the chart in Figure 1 is often used successfully with the basic CPT data of $q_c$ and $f_s$ in most soils (i.e. $q_c$ used in equation 1). Since soils are essentially frictional and both strength and stiffness increase with depth, normalized parameters are more consistent with in-situ soil behavior. The chart in Figure 1 is often referred to as the *Robertson SBTn* chart.

Since 1990 there have been other CPT soil behavior type charts developed (e.g. Jefferies and Davies, 1991; Olsen and Mitchell, 1995; Eslami and Fellenius, 1997; Ramsey, 2002; Schneider et al, 2008; Schneider et al, 2012). Each chart tends to have advantages and limitations some of which were briefly discussed by Robertson (2009). A common feature in many of these CPT-based methods is that the classification system uses groupings based on traditional physical descriptions (e.g. sand and clay) even though the methods are based on behavior measurements (e.g. either $q_c$ or $q_t$ and $f_s$). This has resulted in some confusion in geotechnical practice.

Jefferies and Davies (1993) identified that a Soil Behavior Type Index, $I_c$, could represent the SBTn zones in the $Q_{t1}$ - $F_r$ chart where $I_c$ is essentially the radius of concentric circles that define the boundaries of soil type. Robertson and Wride, (1998) modified the definition of $I_c$ to apply to the Robertson (1990) $Q_{t1} - F_r$ chart, as defined by:

$$I_c = [(3.47 - \log Q_{t1})^2 + (\log F_r + 1.22)^2]^{0.5} \quad (4)$$

The contours of $I_c$ can be used to approximate the SBTn boundaries. The circular shape of the $I_c$ boundaries provides a reasonable fit to the SBTn boundaries in the center of the chart where much of the data exists for most normally to lightly overconsolidated *'ideal soils'*. For some soils, the circular shape is a less effective fit to the original SBT boundaries, as illustrated in Figure 1 for $I_c = 2.6$ and discussed by Robertson (2009). Robertson and Wride (1998) had suggested that $I_c = 2.6$ was an approximate boundary between soils that were either more sand-like or more clay-like, based on cyclic liquefaction case histories that were limited to predominately silica-based *'ideal soils'* that were essentially normally consolidated. However, experience has shown that the $I_c = 2.6$ boundary is not always effective in soils with significant microstructure.

Robertson (2009) updated the normalized cone resistance and the associated SBTn chart, using a normalization with a variable stress exponent, n; where:

$$Q_{tn} = [(q_t - \sigma_v)/p_a](p_a/\sigma'_{vo})^n \quad (5)$$

where: $(q_t - \sigma_v)/p_a$ = dimensionless net cone resistance
$(p_a/\sigma'_{vo})^n$ = stress normalization factor
$p_a$ = atmospheric reference pressure in same units as $q_t$ and $\sigma_v$
n = stress exponent that varies with SBTn, and defined by;

$$n = 0.381\ (I_c) + 0.05\ (\sigma'_{vo}/p_a) - 0.15 \quad (6)$$

where $n \leq 1.0$

The chart shown in Figure 1 uses $Q_{tn}$, instead of the original $Q_{t1}$ suggested by Robertson (1990), and where $I_c$ is also determined using $Q_{tn}$ (Robertson, 2009). In most fine-gained soils when $I_c > 2.6$, $Q_{t1} \sim Q_{tn}$ since $n \sim 1.0$. Likewise, when $\sigma'_{vo}$ = 1atm (100kPa) and $\sigma'_{vo}$ > 10atm (1MPa), $Q_{t1} = Q_{tn}$. The largest difference between $Q_{t1}$ and $Q_{tn}$ occurs in coarse-grained soils at shallow depth ($\sigma'_{vo}$ < 1atm), when $Q_{t1} > Q_{tn}$, (since $n < 1.0$). Jefferies and Been (2006) had suggested that the stress exponent in equation 5 should always be n = 1.0. However, due to the non-linear variation of shear stiffness (G) with depth, the effective stress exponent in coarse-grained soil can be less than 1.0, as indicated by equation 6.

The original method suggested by Robertson (1990) included a chart based on $Q_{t1}$ and $B_q$. However, Schneider et al (2008) showed that $B_q$ may not be the best form of normalized CPT pore pressure to identify soil type and suggested a chart based on $Q_{t1}$ and $U_2$ (where $U_2 = \Delta u_2/\sigma'_{vo}$). The Schneider et al (2008) pore pressure chart applies mostly to clay-like soils since it requires a measured excess penetration pore pressure ($\Delta u_2$) and was developed primarily to aid in separating whether CPT penetration is drained, undrained or partially drained. The Schneider et al (2008) $Q_{t1} - U_2$ chart uses slightly different grouping of soil type (and description terms) compared to the Robertson (1990) chart, which can also lead to some confusion when applying both.

There is now more than 25years experience using the *Robertson SBTn* chart and in general, the chart provides good agreement between USCS-based classification and CPT-based SBTn (e.g. Molle, 2005) for most soils with little microstructure. Robertson (2009) discussed several examples where there can be observed

differences. In summary, the *Robertson SBTn* chart tends to work well in *'ideal soils'* (i.e. unstructured soils) but can be less effective in *'structured soils'*. Schneider et al (2012) and Saye et al (2017) suggested adjusting the boundaries to be more hyperbolic in shape so that they are steeper in the region of higher $F_r$ values. Based on the accumulated experience using the SBTn chart it is possible to update the chart and to modify the descriptions of 'soil type' to use terms based more on soil behavior. It is also possible to identify soils with significant microstructure using additional CPT-based measurements (e.g. SCPT).

# 5 PROPOSED MODIFIED SBTN CHARTS

As discussed in the section on soil behavior, a major factor in any classification system can be the effects of post deposition processes that can generate microstructure. Hence, it can be important to first identify if soils have significant microstructure, since this can influence the in-situ behavior and ultimately the effectiveness of any classification system based on in-situ tests. Some understanding of the geologic background of the soil is always a required starting point for reliable classification based on CPT data, since geology provides a framework for interpretation.

The combined information from the SCPT has the potential to aid in identification of possible microstructure in soils to either supplement existing geologic information or when geologic information maybe either lacking or uncertain. Eslaamizaad and Robertson (1996) and Schnaid (2009) suggested that the SCPT can be helpful to identify soils with microstructure based on a link between $G_o/q_t$ and $Q_{tn}$, since both aging and bonding tend to increase the small strain stiffness ($G_o$) significantly more than they increase the large strain strength of a soil (reflected in both $q_t$ and $Q_{tn}$). Hence, for a given soil, age and bonding both tend to increase $G_o$ more than the larger strain cone resistance ($q_t$), all other factors (in-situ stress state, etc.) being constant. Schneider and Moss (2011) extended the link between CPT and $G_o$ to establish a method to identify sandy soils with microstructure. Schneider and Moss (2011) suggested using an empirical parameter, $K_G$ defined in equation 7 (modified from Rix and Stokoe, 1991):

$$K_G = (G_o/q_t)\,(Q_{tn})^{0.75} \tag{7}$$

where $G_o$ is in same units as $q_t$ and $Q_{tn}$ is dimensionless:
$G_o$ = small strain shear modulus = $\rho\,(V_s)^2$
$V_s$ = shear wave velocity
$\rho$ = soil mass density = $\gamma/g$
$\gamma$ = soil unit weight
g = acceleration due to gravity

Schnaid (2009) and Robertson (2009) proposed similar relationships but with slightly different exponents for $Q_{tn}$. The ratio $G_o/q_t$ is essentially a small strain rigidity index ($I_G$), since it defines stiffness to strength ratio, where $G_o$ is the small strain stiffness and $q_t$ is a measure of soil strength. Robertson (2015) had suggested that $K_G$ is essentially a normalized rigidity index, since it normalizes the small strain rigidity index ($G_o/q_t$) with in-situ soil state reflected by $Q_{tn}$. The works by Eslaamizaad and Robertson (1996), Schnaid (2009) and Schneider and Moss (2011) were focused primarily on coarse-grained soils. Robertson (2009) suggested that the small strain rigidity index ($I_G$) can be extended to include fine-grained soils and should be defined based on net cone resistance $q_n$, since $q_n$ is a more correct measure of soil strength, to be:

$$I_G = G_o/q_n \tag{8}$$

where $q_n = (q_t - \sigma_v)$

Hence, a modified normalized small strain rigidity index, $K^*_G$ is defined as:

$$K^*_G = (G_o/q_n)\,(Q_{tn})^{0.75} \tag{9}$$

Figure 2 presents a plot of $Q_{tn}$ versus $I_G$ similar to that shown by Schneider and Moss (2011) but extended to cover a wider range of soils. Schneider and Moss (2011) showed that most young, uncemented (*ideal*) silica-based sands have $100 < K_G < 330$, with an average value of around 215. In most coarse-grained soils $q_t \sim q_n$ since $q_t > \sigma_v$, hence the data presented by Schneider and Moss (2011) in terms of $K_G$ also plot in the same region in terms of $K^*_G$ on the modified plot shown in Figure 2. Since Figure 2 has been extended to include

soft clays the modification to use $G_o/q_n$ becomes important, since $q_n$ is a direct measure of soil strength in clay-like soils and can be significantly smaller than $q_t$ in soft clay.

Most of the existing empirical correlations developed for interpretation of CPT results are predominately based on experience in silica-based soils with little or no microstructure (e.g. Robertson, 2009; Mayne, 2014). Hence, if soils have $K^*_G < 330$ the soils are likely young and uncemented (i.e. have little or no microstructure) and can be classified as '*ideal soils'* (unstructured) where many traditional CPT-based empirical correlations likely apply. Soils with $K^*_G > 330$, tend to have significant microstructure and the higher the value of $K^*_G$, the more microstructure is likely present. Hence, if a soil has $K^*_G > 330$ the soils can be classified as '*structured soils'* where traditional generalized CPT-based empirical correlations may have less reliability and where local modification may be needed. The influence of increasing microstructure on in-situ soil behavior is often gradual and any separating criteria can be somewhat arbitrary. Data suggests that very young uncemented soils tend to have $K^*_G$ values closer to 100, whereas soils with some microstructure (e.g. older deposits) tend to have $K^*_G$ values closer to 330. As will be shown later, soils with $K^*_G < 330$ tend to have little or no microstructure where existing empirical CPT-based correlations tend to provide good estimates of soil behavior.

A challenge when calculating $K^*_G$, that will be illustrated later, is that the CPT parameters ($q_t$ and $Q_{tn}$) and $V_s$ are often measured over different depth intervals. For example, CPT measurements are typically made at 10 to 50mm depth intervals, whereas $V_s$ (and hence, $G_o$) is typically measured over 500 to 1000mm (or larger) depth intervals. Hence, there can be a scale effect when combining the two parameters ($G_o/q_n$), where the CPT parameters respond to smaller features and variability in the ground and $V_s$ (and $G_o$) tend to respond in a more subdued average manner. In the examples shown later, the CPT data ($q_n$) was averaged over the depth interval that was used to obtain the $V_s$ measurement (e.g. if $V_s$ was taken at 1m intervals, the associated $q_n$ value was taken as the average value over the same 1m interval). Hence, the calculated value of $K^*_G$ can show some variability in non-homogenous soils.

Natural soils can also be anisotropic where the small strain stiffness can vary depending on the direction of loading where $G_{oVH}$ (and $V_{sVH}$) may not be equal to $G_{oHH}$ (and $V_{sHH}$). The subscript VH applies to stiffness that is measured in the vertical and horizontal direction, which is the most commonly measured in-situ shear wave velocity ($V_{sVH}$), i.e. either a vertically propagating wave with particle motion in the horizontal direction ($V_{sVH}$) or a horizontal propagating wave with particle motion in the vertical direction ($V_{sHV} = V_{sVH}$). The suggested relationship shown in Figure 2 is based on $G_{oVH}$ (and $V_{sVH}$) that is measured primarily using the SCPT. For simplicity, the relationship is shown in terms of $G_o$ but is intended to apply $G_{oVH}$.

Robertson (2009) presented contours of state parameter ($\psi$) for young uncemented coarse-grained (*unstructured*) soils on the normalized SBTn ($Q_{tn} - F_r$) chart and suggested that the contour for $\psi < -0.05$ could be used to separate coarse-grained *'ideal soils'* that are either contractive or dilative at large strains. This was supported by case histories where flow liquefaction had occurred (Robertson, 2010).

Robertson (2009), Mayne (2014) and others have shown that most fine-grained *'ideal soils'* with an OCR > 4 should have $Q_{tn} > 12$ and are predominately dilative at large shear strains. Hence, combining these two criteria it is possible to develop a simple $Q_{tn} - F_r$ based boundary that would separate *'ideal soils'* that are either contractive or dilative at large shear strains, as shown on Figure 3 by the solid line (marked CD = 70). The contractive-dilative (CD) boundary can be represented by the following simplified expression:

$$CD = 70 = (Q_{tn} - 11)(1 + 0.06\ F_r)^{17} \qquad (10)$$

When CD > 70 the soils are likely dilative at large shear strains, as shown on Figure 3. Equation 10 is a simplified fitting relationship to capture the generalized shape of the contractive-dilative boundary on the $Q_{tn} - F_r$ chart. Figure 3 also includes (as light dashed lines) the original SBTn boundaries suggested by Robertson (1990, 2009) for comparison and to retain the original grouping based on physical characteristic descriptions (e.g. sand and clay). Because Figure 3 shows behavior based descriptions and boundaries, it applies primarily to soils that have little or no microstructure (i.e. *'ideal soils'*).

A CPT-based boundary between contractive and dilative soils depends on many variables (e.g. in-situ stress state, soil plastic hardening) and there is a transition between *'ideal soils'* that are predominately contractive to soils that are predominately dilative at large shear strains. Robertson (2010) indicated that the flow liquefaction case histories showed that the suggested boundary (represented by CD = 70) was slightly conservative (i.e. soils with some data slightly lower $Q_{tn}$ values could be dilative at larger strains). The dashed line in Figure 3 shows an approximate lower limit, based on the case histories presented by Robertson (2010) for *'ideal soils'* that are predominately dilative at large strains that can be represented by the following simplified expression:

$$CD \text{ (lower bound)} = 60 = (Q_{tn} - 9.5)(1 + 0.06\ F_r)^{17} \quad (11)$$

In general, it is recommended to apply the upper boundary (CD = 70) for most geotechnical interpretation, since this is often slightly conservative. The CD = 70 boundary shown in Figure 3 applies only to *'ideal soils'* with little or no microstructure, since some aged and/or cemented soils can be contractive at large strains but produce relatively high values of $Q_{tn}$ due to the increased stiffness and strength from aging and/or cementation. Examples will be presented later to illustrate this point.

The boundary between the original (Robertson, 1990) SBTn zones 4 (silt-mixtures) and 5 (sand-mixtures) is the approximate boundary between soils that are either more clay-like or more sand-like and can be approximated by $I_c = 2.6$ (Figure 1). However, the simple circular shape of $I_c$ is not always a good fit to the original boundary, except for predominately young uncemented, essentially normally consolidated (*ideal*) soils, as suggested by Robertson and Wride (1998).

Schneider et al (2012) had suggested a more hyperbolic shape (in terms of log $Q_t$ and log $F_r$) to better capture the SBT boundaries. Figure 3 shows suggested modified main SBTn boundaries based on a more hyperbolic shape using a Modified Soil Behavior Type Index, $I_B$, defined as:

$$I_B = 100(Q_{tn} + 10) / (Q_{tn}\ F_r + 70) \quad (12)$$

The boundary shown on Figure 3 represented by $I_B = 32$ represents the lower boundary for most sand-like *'ideal soils'* and is similar to the original boundary between SBTn zones 4 and 5 for normally consolidated soils. The boundary represented by $I_B = 22$ represents the upper boundary for most clay-like *'ideal soils'*, and is similar to the original boundary between SBTn zones 3 and 4 for normally consolidated soils. The value of $I_B = 22$ represents the approximate boundary for a plasticity index PI ~ 18% in fine-grained *'ideal soils'*.

The region represented by $22 < I_B < 32$ is defined as *'transitional soil'* which are soils that can have a behavior somewhere between that of either sand-like or clay-like *'ideal soil'* (e.g. low plasticity fine-grained soils, such as silt). Some *'transitional soils'* can also respond in a partially drained manner during the CPT (e.g. DeJong and Randolph, 2014) and are sometimes referred to as '*intermediate soils'*. The modified boundaries shown in Figure 3 are similar to the original boundaries for zones 3, 4 and 5 in the central part of the chart, where most young uncemented, normally consolidated *'ideal soils'* plot.

The soil close to the friction sleeve of the cone has experienced very large shear strains and tends to be fully '*destructured*' and/or remolded. Based on this observation, Robertson (2009) had suggested that sensitivity ($S_t$) in most fine-grained *'ideal soils'* could be estimated using the simplified expression:

$$S_t = 7.1 / F_r \quad (13)$$

Hence, soils with $F_r < 2\%$ tend to have a sensitivity $S_t > 3$ to 4. This boundary has been included in Figure 3 as an approximate separation between clay-like-contractive (CC) soils with moderate to low sensitivity ($S_t < 3$) from clay-like-contractive soils with higher sensitivity, $S_t > 3$ (CCS). This value of sensitivity is somewhat conservative but considered appropriate for basic classification purposes. Any boundary based on sensitivity is somewhat arbitrary, but can be helpful to warn users when a soil may have higher sensitivity to disturbance with associated risk of strength loss. As shown in Figure 3 the boundary between CC and CCS is slightly more conservative than the previous boundary suggested by Robertson (1990).

Eslami and Fellenius (1997) had suggested that charts based on $Q_t$ and $F_r$ were not mathematically correct for any statistical analyses since both $Q_{tn}$ and $F_r$ use $q_t$. Figure 4 shows the same boundaries as Figure 3 but represented on a modified SBTn chart based on $Q_{tn}$ and F (where F is the normalized sleeve resistance, $F = f_s/\sigma'_{vo}$). Figure 4 (dashed lines) shows the original boundaries suggested by Robertson (1990), for comparison. The format shown in Figure 4 has the advantage that the normalized parameters are independent, but the disadvantage that data becomes more compressed. For most applications, there is no difference between Figures 3 and 4 and either format can be used, although the $Q_{tn} – F_r$ format (Figure 3) is preferred and for the examples shown later, this format is used. Figure 4 is similar to the earliest normalized CPT 'characterization' chart that was suggested by Olsen (1984).

The $Q_{tn} – F_r$ chart can also be used when no pore pressure ($u_2$) data are available (i.e. basic CPT data), since $q_c \sim q_t$ for most soils, except soft fine-grained soils ($Q_{t1} < 10$). Although the basic $Q_{tn} – F_r$ charts tend to be more popular for most onshore projects, since they do not require accurate CPT pore pressure measurements, it can be helpful to include CPT measured pore pressures into the interpretation of soil behavior type. Since Schneider et al (2008) showed that a slightly better form for the normalized pore pressure is $U_2$, Figure 5 shows a proposed modified Schneider et al (2012) chart using the same behavior type terms applied in Figure 3 but using the generalized normalized cone resistance, $Q_{tn}$, instead of $Q_{t1}$. The equations to define the boundaries shown in Figure 5 were provided by Schneider et al (2008) but replacing $Q_{t1}$ with $Q_{tn}$. For most clay-like soils there is little difference between $Q_{tn}$ and $Q_{t1}$, since $n \sim 1.0$, but for consistency it is preferred to use $Q_{tn}$. Pore pressures measured in the $u_2$ location (just behind the cone tip) are dominated by soil behavior in shear at large strains, hence $U_2$ tends to reflect the behavior of the soil in shear at large strain (i.e. destructured). In general, positive $U_2$ values tend to reflect large strain contractive behavior and negative $U_2$ values tend to reflect large strain dilative behavior. Hence, mostly 'contractive' behavior descriptions are shown on Figure 5 for positive values of $U_2$. Based on the $Q_{tn} – F_r$ chart (Figure 3), most fine-grained *'ideal soils'* with $Q_{tn} > 12$ will have negative values of $U_2$ since they are generally dilative at large shear strains. However, *'structured soils'* can have $Q_{tn} > 12$, due to the increased strength and stiffness, combined with large positive values of $U_2$ due to the loss of structure resulting in a contractive behavior at large strains. Hence, if data plot in the region represented by $Q_{tn} > \sim 12$ combined with high positive $U_2$ values ($U_2 > 4$), the soils likely have significant microstructure (i.e. '*structured soils'*) and are contractive at large shear strains. Increasing values of $Q_{tn}$ combined with increasing positive $U_2$ values indicate increasing microstructure, as indicated in Figure 5. This will be illustrated later with some examples. Schneider et al (2008) showed that soils with increasing coefficient of consolidation ($c_v$) tend to show a decrease in $U_2$ with increasing $Q_{tn}$, due in part to an increase in drainage during the CPT but also an increased tendency for dilative behavior. For a given soil, increasing OCR can be associated with increasing $c_v$, hence *'ideal soil'* with increasing OCR tend to show a decrease in $U_2$ combined with an increase in $Q_{tn}$, as illustrated in Figure 5.

The $Q_{tn} – F_r$ chart has a modified SBTn Index $I_B$ that can be used to define the main boundaries in soil SBTn. Likewise, the $Q_{tn} – U_2$ chart can use $B_q$ as an approximate SBTn index to define the main boundaries, as shown in Figure 5. Hence, soils with $0.2 < B_q < 0.6$ tend to be CC and soils with $0.6 < B_q < 1.0$ and $Q_{tn} > 4$ tend to be CCS, as shown in Figure 5. Likewise, soils in the region defined by $U_2 > 0$ with $Q_{tn} = 20$ and $U_2 > 10$ with $Q_{tn} = 10$ appear to have significant microstructure. The combination of $Q_{tn} – F_r$ (Figure 3) and $Q_{tn} – U_2$ (Figure 5) can aid in identification of soils with microstructure since '*structured soils'* tend to have different classification between the two charts.

A major challenge for any classification method based on CPT pore pressures is the risk that the measured pore pressures may be unreliable due to loss of saturation (Robertson, 2009). This is an issue for CPT profiles performed onshore either in soils that are dilative or when the water table is deep and the cone is required to penetrate unsaturated and/or dilative soils for some depth.

Ideally, the above three charts (Figures 2, 3 and 5) should be used together to improve soil classification. Figure 2 ($Q_{tn} - G_o/q_n$) can be used to identify soils with significant microstructure (e.g. age and/or cementation), i.e. $K^*_G > 330$, provided $V_s$ data are available. If the soils have little or no microstructure (i.e. '*ideal soil'*), Figure 3 ($Q_{tn} – F_r$) should apply. Figure 5 ($Q_{tn} – U_2$) can be used primarily in fine-grained soils, when $V_s$ data are either not available or as a supplement to Figure 3, to evaluate if soils have significant microstructure and to evaluate large strain behavior, provided reliable pore pressure measurements are made.

The following section will illustrate the main features of the above approach using mostly published SCPTu data from well-documented sites. Schneider and Moss (2011) have essentially demonstrated the effectiveness of the $Q_{tn} - G_o/q_t$ chart for a wide range of coarse-grained soils and Schneider et al (2008) have essentially demonstrated the effectiveness of the $Q_{tn} - U_2$ chart for a wide range of fine-grained soils, hence the focus will tend to be more on the $Q_{tn} - F_r$ chart, although data will be presented on all three charts for each example site.

# 6 CASE HISTORY EXAMPLES

Selected representative case histories are presented to identify specific features that illustrate key points. Table 1 presents a summary of the selected deposits used to evaluate the proposed modified SBTn charts. The sites shown in Table 1 were selected to represent a wide range of deposits ranging from very recent fill and/or tailings to older very stiff soil/soft rock. The deposits have been listed by increasing value of $K^*_G$ that essentially capture increasing microstructure. SCPTu data will be presented in the three normalized charts ($Q_{tn}$–$F_r$; $Q_{tn}$–$U_2$ and $Q_{tn}$–$I_G$).

Figure 6, 7 and 8 presents a summary of the average values for all the case history example deposits on the $Q_{tn}$–$I_G$, $Q_{tn}$–$F_r$ and $Q_{tn}$–$U_2$ charts, respectively. Figure 6 ($Q_{tn}$–$I_G$) shows that the value of $K^*_G = 330$ suggested by Schneider and Moss (2011) provides a good separation between soils with little or no microstructure and soils with significant microstructure. Also, $K^*_G = 330$ appears to separate predominately silica-based soils from carbonate-based soil. Figure 7 ($Q_{tn}$–$F_r$) shows that, in general, soils with significant microstructure tend to plot in the dilative region of the chart. Figure 8 ($Q_{tn}$–$U_2$) shows that fine-grained contractive soils with significant microstructure plot in a region defined approximately by $U_2 > 0$ when $Q_{tn} = 20$ and $U_2 > 10$ when $Q_{tn} = 10$.

The following examples were selected to illustrate the variation and trends in the SCPTu data in the selected deposits.

## 6.1 SOILS WITH LITTLE OR NO MICROSTRUCTURE

Figure 9 shows SCPTu data to a depth of 40m at the KIDD site near Vancouver, BC, that was part of the CANLEX research project (Robertson et al, 2000, Wride et al., 2000). The soils are essentially normally consolidated, uncemented Holocene-age natural (silica-based) deposits from the Fraser River delta and represent both sand-like and clay-like soils in one profile. The SCPTu was carried out at a part of the site where the soils from a depth of about 4 to 22.7m are relatively uniform medium dense fine sand overlying uniform sensitive marine clay with the water table at a depth of 1m and $V_s$ measurements were made every 0.5m starting at 3.25m. The sand (4 to 22.7m) plots predominately in the sand-like-dilative (SD) region consistent with the detailed results from the CANLEX project with an average $K^*_G = 214$. The underlying normally consolidated sensitive marine clay (22.9 to 40m) plots in the clay-like-contractive-sensitive (CCS) region on both the $Q_{tn}$ - $F_r$ and $Q_{tn}$ - $U_2$ charts, with an average $K^*_G = 215$. The $K^*_G$ values are consistent with the Holocene-age with no evidence of cementation. Figure 9 shows that the original descriptions used by Robertson (1990) also provide a good classification of both the sand and clay deposits. The CPT data transitions from the sand to the clay between 22.7 and 22.9m and is incorrectly classified. The issue of data in transition from sand-like to clay-like was discussed by Robertson (2009).

Figure 10 shows SCPTu data to a depth of 35m at a site in the San Francisco Bay area near Vallejo. The test location was pre-drilled using a hand auger to a depth of 1.5m after which the SCPTu was started and $V_s$ measurements were made every 1m starting at a depth of 2m. The groundwater table is at a depth of 2m. The site is composed of about 1.5m of fill overlying Young Bay Mud (YBM) to a depth of around 12m. General details about YBM are provided by Bonaparte & Mitchell (1979). At this location, the YBM is late Holocene-age and lightly overconsolidated below a depth of 4m (OCR < 1.5) with a desiccated surface crust due to groundwater fluctuations. Below the YBM is Old Bay Clay (OBC) to the final depth of the SCPTu at 36m. SCPTu data from 2 to 11m in the YBM are shown in Figure 10a and from 12 to 35m in the OBC on Figure 10b. The average $K^*_G$ value for the YBM at this site is around 85 consistent with the young geologic age and lack of microstructure. The OBC has slightly higher $K^*_G$ values of around 300 consistent with the older geologic age (late Pleistocene). The YBM below the desiccated crust plots in the clay-like-contractive-sensitive (CCS) region on the $Q_{tn} - F_r$ chart and in the clay-like-contractive (CC) region of the $Q_{tn} - U_2$ chart. The YBM has a sensitivity of around 4 to 6 based on field vane tests that is consistent with the classification of CCS. The difference in classification between the $Q_{tn} - F_r$ and $Q_{tn} - U_2$ charts is partly due to a somewhat

slow pore pressure response in the upper 11m of the profile after recording small negative pore pressures in the desiccated crust. In the YBM desiccated crust the normalized cone resistance ($Q_{tn}$) moves higher and plots in the transitional soil region (TC and TD) of the $Q_{tn} - F_r$ chart. As desiccation increases closer to the ground surface, with associated increase in apparent OCR, the CPT data plots higher on both the $Q_{tn} - F_r$ and $Q_{tn} - U_2$ charts. As Schneider et al (2008) identified the $U_2$ values decrease with increasing $Q_{tn}$ due to a more dilative behavior and increasing $c_v$ (and possible partial drainage during the CPT). Close to the ground surface (at a depth of about 2m) some of the SCPTu data plot in the sand-like-dilative (SD) region due in part to the very dilative behavior of the very stiff desiccated clay and the almost drained penetration during the CPT, however, most of the SCPTu data for the desiccated crust plot in the transitional-dilative (TD) region. The OBC is more stratified and variable as indicated by the wide range in normalized CPT values shown in Figure 10b. Much of the OBC data plot on the boundary between clay-like and transitional soils and contractive to dilative behavior, consistent with the variable nature of this predominately stiff overconsolidated sandy clay.

Figure 11 shows SCPTu data from the Madingley site near Cambridge, UK (Lunne et al, 1997) from 2 to 12m. The Madingley site is underlain by Gault clay that is very stiff overconsolidated fissured clay of the Cretaceous period (~110 million years ago) with OCR > 10. The high overconsolidation ratio is derived from significant stress removal with no evidence of cementation. The SCPTu data correctly plot predominately in the clay-like-dilative (CD) region of the $Q_{tn} - F_r$ chart but plot close to the sand region of the $Q_{tn} - U_2$ chart, due to the negative values of $U_2$. This trend of small or negative $U_2$ values was illustrated in Figure 6 for 'ideal soils' with high OCR. The average $K^*_G = 360$ indicates some microstructure consistent with the significant age of the deposit but no cementation. The $K^*_G$ value of 360 puts this clay close to the boundary between a soil with little or no microstructure and a soil with significant microstructure. Given that the existing empirical correlations provide a reasonably good estimation of soil behavior (Lunne et al, 1997), the clay can be considered to be close to the limit of the suggested boundary for *'ideal soils'*.

The above examples, where $K^*_G < 330$, were soils with little or no microstructure and where the proposed SBTn charts provided general good classification in terms of behavior type.

### 6.2 SOILS WITH SIGNIFICANT MICROSTRUCTURE

The following examples illustrate soils with significant microstructure, where $K^*_G > 330$ and where the CPTu data does not always fit well on the SBTn charts.

Figure 12 shows SCPTu data to a depth of 50m at the Cooper River Bridge site in Charleston, SC, (Camp et al, 2002) where the soil below a depth of 22m is Cooper Marl, that is a stiff calcareous plastic clay or silt of Eocene to Oligocene-age (~30 to 40 million years ago). The SCPTu data from 22 to 50m plot predominately in the transitional-contractive (TC) region of the $Q_{tn}$–$F_r$ chart and the clay-like-contractive (CC) region of the $Q_{tn}$–$U_2$ chart with an average $K^*_G = 580$. Dissipations tests provided $t_{50}$ values ranging from 90 to 850s that indicate predominately undrained cone penetration. Data from a nearby site in the same Cooper Marl but at a shallow depth (less than 9m) have higher values of $Q_{tn} > 40$ and plot more in the SC and SD regions and with values of $U_2$ as high as 50. The high $K^*_G$ and $U_2$ values indicate significant microstructure consistent with cementation from the high carbonate content (Camp et al, 2002). The high $Q_{tn}$ values suggest a relatively high apparent OCR (>4) and possible dilative behavior whereas the high $U_2$ values show a more contractive behavior at high shear strains consistent with a cemented soil. The high level of cementation is consistent with a very stiff behavior at small strains followed by a contractive behavior at high shear strains when the cementation is broken and the soil becomes destructured.

Figure 13 shows SCPTu data from a site in Atlanta, Georgia in the Piedmont residual soil (Mayne, 2009). The site served as a test area for instrumented piles (Harris and Mayne, 1994) and consists of silty fine sand derived from the weathering of the underlying gneiss and schist bedrock. The SCPTu data from 4 to 19m plot predominately on the boundary between sand-like-dilative (SD) and transitional-dilative (TD) region of the $Q_{tn}$–$F_r$ chart with an average $K^*_G = 520$. The excess pore pressures are generally negative with values close to -100kPa and hence close to the saturation limit of the sensor. Dissipations tests provided $t_{50}$ values ranging from 20 to 100s that indicate a potentially partially drained cone penetration. The negative pore pressures and the potential for partially drained penetration can explain why the data plot toward the sand region of the $Q_{tn}$-$U_2$ chart. The high $K^*_G$ values indicate significant microstructure consistent with the remaining cementation in the residual soil. Residual soils derived from granite bedrock in Porto, Portugal have similar high $K^*_G$

values and plot in TD region of the $Q_{tn}$–$F_r$ chart whereas data from a fine grained clayey silt residual soil in Campinas, Brazil plot in the CD region of the $Q_{tn}$–$F_r$ chart (De Mio et al, 2010). The significant microstructure present in many residual soils tends to explain why the current SBTn charts often misinterpret their classification.

Figure 14 shows SCPTu data from a site near downtown Los Angeles composed of a uniform siltstone from 3 to 10m. The siltstone is part of the Fernando formation of Pliocene age (~3 to 5 million years ago). The SCPTu data plot in the sand-like-dilative region (SD) on the $Q_{tn}$–$F_r$ chart but in the clay-like-contractive (CC) region of the $Q_{tn}$–$U_2$ chart (note that the $U_2$ values are between 18 to 40 and are mostly off the scale of the $Q_{tn}$–$U_2$ chart at the scale shown). The average $K^*_G = 635$ is consistent with the old age of the deposit combined with the cemented nature of this soft rock. The $Q_{tn}$–$U_2$ chart is correctly classifying the behavior as contractive at large strain that is different to the dilative behavior suggested by the $Q_{tn}$–$F_r$ chart. The difference is explained by the significant microstructure (cementation) identified by the high $K^*_G$ values.

Figure 15 shows SCPT data from a site in Tangiers, Morocco (Debats et al, 2015) composed of hydraulically placed calcareous sand. The sand has a high carbonate content ranging from 75 to 95% and is composed of shell fragments and carbonate algae mixed with grains of silica and mica (Debats et al, 2015). The highly compressible nature of the carbonate (shell) mineralogy produces small friction ratio values ($F_r < 0.3\%$) but high small strain stiffness with $K^*_G \sim 380$. Soils with high carbonate content have a tendency to develop rapid calcium cementation resulting in some microstructure and high values of $K^*_G$. However, it is also possible that an apparent microstructure is caused by the highly compressible nature of the carbonate grains. The resulting 'microstructure' often makes CPT interpretation difficult using traditional empirical correlations based on predominately silica-based soils.

In some parts of the middle east where calcareous sands exist it has become common practice to correct the CPT cone resistance to 'equivalent silica-sand' values using a Shell Correction Factor (SCF) where:

$$q_{c(ss)} = SCF\ q_c \tag{14}$$

where $q_{c(ss)}$ = equivalent silica-sand cone resistance

The SCF has been estimated based on calibration chamber studies that have been costly and provide limited results. Debats et al (2015) suggested that the SCF could be estimated from SCPT data by adjusting $q_c$, using an iterative approach with variable SCF values, until the measured $V_s$ agrees with an estimated $V_s$ using the empirical CPT-based correlation suggested by Robertson (2009) using the adjusted $q_c$. Since the average $K^*_G$ for most young, uncemented silica-based sands is about 215 (Schneider and Moss, 2011), it is also possible to estimate the SCF based on SCPT data using the following simplified relationship:

$$SCF = (K^*_G/215)^{1.334} \tag{15}$$

where $K^*_G$ = the average measured normalized small strain rigidity index.

Application of equation 15 is conceptually similar to the approach used by Debats et al (2015) but avoids the need for iteration to obtain the SCF. For the data shown in Figure 15, the SCF based on equation 15 is 2.1 compared to the average value of about 2.0 suggested by Debats et al (2015).

# 7 DISCUSSION

The above examples illustrate that the modified $Q_{tn}$–$F_r$ and $Q_{tn}$–$U_2$ charts provide good classification in terms of soil behavior type for soils with little or no microstructure when $K^*_G < 330$. The $Q_{tn}$–$U_2$ chart can be somewhat sensitive to minor loss of saturation of the pore pressure sensor in some soils, especially in stiffer onshore soils. In soils and soft rock where there is significant microstructure (i.e. *'structured'* soils) with $K^*_G > 330$ the classification of soil behavior type becomes less reliable and some judgment is required. If *'structured'* soils and/or soft rocks are sufficiently fine-grained to develop reliable excess pore pressures, the $Q_{tn}$–$U_2$ chart provides a better classification of soil behavior type at large strains and can be used to identify significant microstructure. Geomaterials with significant microstructure tend to be cemented/bonded and can

be very stiff at small strains (producing high $Q_{tn}$ values) but can be contractive at large shear strains (producing high $U_2$ values) when the cementation is destroyed and the material becomes destructured.

As discussed by Robertson (1990) the addition of dissipation tests to measure the rate of dissipation of any excess pore pressures (e.g. $t_{50}$) can also aid in the correct classification of soil behavior, as well as drainage conditions during the CPT. DeJong and Randolph (2014) suggested that when $t_{50} > 50$s the cone penetration (1000 mm$^2$ cone at standard rate of 20mm/s) is essentially undrained.

Soil behavior is controlled by the in-situ effective stress hence CPT parameters normalized in terms of effective stress can better capture in-situ behavior for classification. However, the normalization process is not always perfect due to uncertainty in estimating in-situ stress. Conceptually, any normalization should also account for the important influence of horizontal effective stresses, since penetration resistance is strongly influenced by the horizontal effective stresses. However, this continues to have little practical benefit for most projects without a prior knowledge of in-situ horizontal stresses (Robertson, 2009). Uncertainty in estimating in-situ vertical stresses can also result from uncertainty in soil unit weight ($\gamma$) as well as the in-situ piezometric profile ($u_o$). This uncertainty typically has a minor effect in coarse-grained soils (e.g. SD and SC) where the measured CPT parameters ($q_c$ and $f_s$) tend to be large relative to $\sigma_{vo}$ and $u_o$. However, the normalized parameters ($Q_{tn}$, $F_r$ and $I_G$) can become sensitive to uncertainty in $\sigma_{vo}$ and $u_o$ in very soft fine-grained soils (e.g. CC and CCS). Likewise, the normalized CPT parameters can also be sensitive to measurement uncertainty in soft fine-grained soil where the measured CPT parameters ($q_c$ and $f_s$) can be close to the limits of accuracy/repeatability for the CPT equipment (Robertson, 2009). One method to identify when the normalized parameters (e.g. $Q_{tn}$ and $F_r$) may not be correct is when the data plot outside some of the limits shown on the charts. For example, $Q_{tn} < 1$ when pushing in soil is rare and is often the result of an overly high estimate for $\sigma_{vo}$. Soft soils with high organic content can have very low soil unit weight that can result in apparent low values of $q_n$ and $Q_{tn}$ due to over-estimated values of $\sigma_{vo}$. In soft fine-grained soil, it is also rare to obtain $B_q > 1.2$, since this requires an excess pore pressure higher than the net cone resistance ($q_n$). Hence, if data plot lower than the line identified by $B_q = 1.0$ in the $Q_{tn} – U_2$ chart, there may be some uncertainty in the low values of $Q_{tn}$. In soft soil, the uncertainties in estimating $\sigma_{vo}$ and $u_o$ often outweigh the uncertainty in horizontal stress ratio ($K_o$), since variations in $K_o$ tend to be captured by the empirical correlations (e.g. OCR). The normalized parameter $I_G$ requires in-situ shear wave velocity measurements that can be difficult to obtain accurately in the upper 1 to 2m and at depths greater than about 50m using a downhole method like the SCPT. Likewise, scatter in $I_G$ can also result from scale effects between the measured $V_s$ and CPT measurements in heterogeneous deposits.

CPT measurements taken over water often require special care to ensure correct data normalization. Typically, CPT work overwater is referenced to the mudline (i.e. point where soil starts), since the effective stress is zero at the mudline and the cone zero load readings are also taken at the mudline. Hence, $\sigma_{vo}$ and $u_o$ are also referenced to mudline (i.e. equivalent to assuming piezometric surface at the mudline). If the CPT zero load readings are taken at the water surface (e.g. for shallow over water work), the cone ($q_t$ and $u_2$) will measure the water pressure when lowered through water (with $f_s \sim 0$). Hence, $\sigma_{vo}$ and $u_o$ must be selected to produce $\sigma'_{vo} = 0$ at the mudline, that may require using the unit weight of water for the section of CPT data in water.

Calculation of $Q_{tn}$ requires an iterative procedure to determine the stress exponent (n) using $I_c$. The proposed modified SBTn chart based on $Q_{tn}$ and $F_r$ contains a modified soil behavior type index ($I_B$) to define the main boundaries between sand-like and clay-like behavior, however it is recommended to continue using $I_c$ in the iterative procedure to determine $Q_{tn}$, since $I_c$ adequately captures the variation of soil behavior to estimate the stress exponent as well as other current applications of $I_c$ (e.g. Robertson, 2009 and Mayne, 2014).

# 8 SUMMARY AND CONCLUSIONS

Updated and modified charts have been proposed to estimate soil behavior type based on either CPT, CPTu or SCPTu data. Ideally these charts should be used in conjunction with the traditional textural-based classification system (e.g. USCS) based on samples. The charts utilize normalized parameters in an effort to capture in-situ soil behavior. New behavior descriptions are suggested in an effort to be consistent with the concept of a behavior type classification. The method is based on CPT (i.e. electric cones of either 500, 1000 or 1500 mm$^2$ area) at the standard penetration rate of 20mm/s. The $Q_{tn}$–$F_r$ chart does not apply to data from a

mechanical CPT, since both the tip and sleeve resistance values from a mechanical CPT can be different than an electric CPT.

Since soil behavior can be complex, it is recommended to apply multiple CPT-based measurements to improve behavior classification. The SCPTu offers the opportunity to obtain anywhere from 3 to 6 independent measurements to improve classification. However, classification is still possible using either 2 ($q_c$ and $f_s$) or 3 ($q_c$, $f_s$ and $u_2$) measurements from the standard CPT or CPTu. Classification based on only 2 measurements ($q_c$ and $f_s$) is generally less reliable and should be limited to predominately silica-based, young, uncemented soil (i.e. *'ideal soil'*). Classification is improved if 3 measurements are used ($q_c$, $f_s$ and $u_2$) especially in more fine-grained soils. Ideally classification should be based on 4 measurements ($q_c$, $f_s$, $u_2$ and $V_s$) since this allows identification of possible microstructure. In fine-grained soils, dissipation tests that provided an added measurement ($t_{50}$) is also valuable and recommended where possible. Dissipation tests in coarse-grained layers, where 100% dissipation can be rapid and cost effective, are recommended so that the correct equilibrium piezometric pressure ($u_0$) can be determined.

The geologic history of the deposit is always a helpful starting point for correct classification. If the geologic history supports the potential that the soils are predominately silica-based, young (i.e. Holocene to Pleistocene-age) and likely uncemented, the basic SBTn charts based on $Q_{tn}$ and $F_r$ will generally provide reliable classification.

The link between behavior characteristics (e.g. strength, stiffness and compressibility) that is reflected in the CPT measurements and physical characteristics (e.g. grain size and plasticity) can be very good in soils with little or no microstructure (i.e. '*ideal soils'*). Hence, it can be important to identify the level of microstructure in a deposit. If $V_s$ (and hence $G_o$) data are available, ideally using SCPT, the proposed $Q_{tn}$–$I_G$ chart can be used to evaluate the level of microstructure in a deposit with supporting evidence from the geologic background. The modified $Q_{tn}$–$U_2$ can also be helpful in fine-grained soils where CPT penetration is essentially undrained.

If soils have little or no microstructure, the proposed SBTn charts and existing empirical correlations (e.g. Robertson, 2009) tend to apply and can provide reasonable estimates of soil behavior. However, if soils have significant microstructure (e.g. $K^*_G > 330$) the proposed SBTn charts and most existing empirical correlations may not always apply and site or geologic specific modifications may be required.

## 9 ACKNOWLEDGMENTS

This research could not have been carried out without the support, encouragement and input from John Gregg, Kelly Cabal and other staff at Gregg Drilling and Testing Inc. The sharing of ideas and data by Prof. Paul Mayne, Prof. Fernando Schnaid, Dr. James Schneider, M. Jefferies and others has also been helpful and is appreciated.

## 10 REFERENCES

Al-Homoud AS. and Wehr W., (2006). Experience of vibrocompaction in calcareous sand of UAE. *Geotechnical and Geological Engineering*; **24**: 757-774.

ASTM-D 2487-11. Standard Method for Classifying Soils for Engineering Purposes (Unified Soil Classification System). ASTM International. www.astm.org.

Atkinson, J.H., (2007). The Mechanics of Soils and Foundations. Taylor & Fancis, London

Bastani, S.A., Silver, P. and Atkinson, D.R., 2014. CPT based settlement prediction over California soft rock, Proceedings of Third International Symposium of Cone Penetration Testing, CPT'14, Las Vegas, Nevada. Gregg Drilling & Testing. www.cpt14.com.

Begemann, H. K. S., (1965). The friction jacket cone as an aid in determining the soil profile. Proceedings of the 6th ICSMFE, Montreal, Vol. 2, 17-20.

Been, K. & Jefferies, M.G., (1985). A state parameter for sands. Géotechnique, 35(2): 99–112

Boggess, R., and Robertson, P.K. (2010). CPT for soft sediments and deepwater investigations. In Proceedings International Symposium on Cone Penetration Testing, CPT'10, Huntington Beach, Calif., paper 1-17.

Boneparte, R. and Mitchell, J.K., (1979). The Properties of San Francisco May Mud at Hamilton Air Force Base, California. Department of Civil Engineering, University of California, Berkeley.

Bray, J.D. & Sancio, R.B. (2006). Assessment of the liquefaction susceptibility of fine grained soils. Journal of Geotechnical and Geoenvironmental Engineering 132 (9): 1165-1177.

Burland, J.B. 1990. On the compressibility and shear strength of natural clays. Géotechnique 40(3): 329–378.

Camp, W.M., Mayne, P.W. and Brown, D.A., (2002). Drilled shaft axial design values: Predicted versus measured response in Calcareous Clay. Proceedings of Deep Foundations, ASCE GSP No. 116, pp. 1518-1532.

Campanella, R. G., Robertson, P. K., and Gillespie, D. (1983). Cone penetration testing in deltaic soils. Can. Geotech. J., 20-1, 23–35.

Debats, J., Pardessus, N., Racinais, J. and Olgun, C. (2015). InSitu determination of the Shell Correction Factor in Carbonate Sands. Proceedings of 6th International Conference on Earthquake Geotechnical Engineering, Christchurch, New Zealand. Paper 742, 9 pages.

DeGroot, D.J. & Lutenegger, A.J. (2003). Geology and engineering properties of Connecticut Valley Varved Clay. Characterization and Engineering Properties of Natural Soils, Vol. 1, Swets and Zeitlinger, Lisse: 695-724.

DeJong, J. T. and Randolph, M., (2014). Influence of partial consolidation during Cone Penetration on estimated soil behavior type and pore pressure dissipation measurements, Journal of Geotechnical and Geoenvironmental Engineering, ASCE, 138(7): 777-788

Douglas, B.J., and Olsen, R.S., 1981. Soil classification using electric cone penetrometer. *In* Proceedings of Symposium on Cone Penetration Testing and Experience, Geotechnical Engineering Division, ASCE. St. Louis, Missouri, October 1981, pp. 209-227.

Di Mio, G., Giacheti, H.L., Viana da Fonseca, A. and Ferreira, C., (2010). CPTu interpretation for stratigraphic logging differences between sedimentary and residual soils. Proceedings of Second International Symposium of Cone Penetration Testing, CPT'10, Huntington Beach, CA. Gregg Drilling & Testing. www.cpt10.com.

Eslaamizaad, S., and Robertson, P.K., (1996). Seismic cone penetration test to identify cemented sands. In Proceedings of the 49th Canadian Geotechnical Conference. St. John's, Newfoundland. September, pp. 352 – 360.

Eslami, A., and Fellenius, B.H., (1997). Pile Capacity by direct CPT and CPTu methods applied to 102 case histories. Canadian Geotechnical Journal, 34(6): 880-898.

Finno, R.J., Gassman, S.L. and Cavello, M. (2000). The NGES at Northwestern Univ., National Geotechnical Experimentation Sites, GSP 93, ASCE, Reston/Virginia, 130-159.

Harris, D.E., and Mayne, P.W., (1994). Axial compression behavior of two drilled shafts in Piedmont residual soils, Proceedings International Conference on Design and Construction of Deep Foundations, Vol. 2 (Orlando), Federal Highway Administration, Washington, D.C., 352-367.

Hight, D. W. and Leroueil, S., (2003). Characterization of soils for engineering purposes. Characterization and Engineering Properties of Natural Soils, Tan et al. (eds.). Swets and Zeitlinger, pp. 255-360.

Idriss, I. M., and Boulanger, R. W., 2008. Soil liquefaction during earthquakes. Monograph MNO-12, Earthquake Engineering Research Institute, Oakland, CA, 261 pp.

Jefferies, M.G., and Davies, M.P., (1993). Use of CPTu to estimate equivalent SPT $N_{60}$. Geotechnical Testing Journal, ASTM, 16(4): 458-468.

Jefferies, M.G. and Been, K., (2006). Soil Liquefaction – A critical state approach. Taylor & Francis, ISBN 0-419-16170-8 478 pages.

Ku, T., Mayne, P. W. and Cargill, E., (2013). Continuous interval shear wave velocity profiling by auto-source and seismic cone tests, Canadian Geotechnical Journal, 50(2): 382-390.

Leroueil, S. 1992. A framework for the mechanical behavior of structured soils, from soft clays to weak rocks. Proc. US-Brazil NSF Geotechnical Workshop on Applicability of Classical Soil Mechanics Principles to Structured Soils, Belo Horizonte: 107–128.

Leroueil, S. and Hight, D.W., (2003). Behavior and properties of natural soils and soft rocks. Characterization and Engineering Properties of Natural Soils, Tan et al. (eds.). Swets and Zeitlinger, pp. 29-253.

Lunne, T., Eidsmoen, T., Gillespie, D., and Howland, J.D., (1986). Laboratory and field evaluation on cone penetrometers. Proceedings of ASCE Specialty Conference In Situ'86: Use of In Situ Tests in Geotechnical Engineering. Blacksburg, ASCE, 714-729

Lunne, T., Robertson, P.K., and Powell, J.J.M., (1997). Cone penetration testing in geotechnical practice. Blackie Academic, EF Spon/Routledge Publ., New York, 1997, 312 pp.

Lunne, T., Long, M., and Forsberg, C.F., (2003). Characterization and Engineering properties of Holmen, Drammen sand. Characterization and Engineering Properties of Natural Soils, Vol. 2, Swets & Zeitlinger, Lisse, pp. 1121-1148.

Mayne, P.W., (2000). Enhanced Geotechnical Site Characterization by Seismic Piezocone Penetration Test. Invited lecture, Fourth International Geotechnical Conference, Cairo University. pp 95-120.

Mayne, P.W., (2005). Integrated Ground Behavior: In-Situ and Lab Tests, Deformation Characteristics of Geomaterials, Vol. 2 (Proc. Lyon), Taylor & Francis, London, pp. 155-177

Mayne, P.W., (2009), Engineering Design using the Cone Penetration Test: Geotechnical Applications Guide. ConeTec Investigation Inc., 165 pages.

Mayne, P.W., (2014), Interpretation of Geotechnical Paramaters from seismic piezocone tests, Proceedings of 3rd International Symposium on Cone Penetration Testing, CPT14, Las Vegas, Nevada, Gregg Drilling & Testing, Inc., www.cpt14.com.

Mayne, P.W. and Pearce, R.A., 2005, Site characterization of Bootlegger Cove Clay for Port of Anchorage, Proceedings of ISFOG, Anchorage.

Mayne, P.W. and Woeller, D.J., (2008), O-Cell response using elastic pile and seismic piezocone tests, Proceedings of the Second British Geotechnical Association International Conference of Foundations – ICOF (2008), Dundee, Scotland, Edited by Brown, M.J., Bransby, M.F., Brennan, A.J. and Knappett, J.A. Published by HIS BRE Press, UK., Vol. 1:235-246.

Molle, J., 2005. The accuracy of the interpretation of CPT-based soil classification methods in soft soils. MSc Thesis, Section for Engineering Geology, Department of Applied Earth Sciences, Delft University of Technology, Report No. 242, Report AES/IG/05-25, December

Olsen, R.S. (1984). Liquefaction analysis using the cone penetration test. Proceedings of 8th World Conference on Earthquake Engineering. Vol. III, Prentice-Hall Inc., Englewoods Cliffs, NJ, 247-254.

Olsen, R.S., and Mitchell, J.K., (1995). CPT stress normalization and prediction of soil classification. Proceedings of the International Symposium on Cone Penetration Testing, Vol.2, Swedish Geotechnical Society, Linkoping, pp. 257-262.

Ramsey, N., 2002. A calibrated model for the interpretation of cone penetration tests (CPTs) in North Sea Quaternary soils. Offshore site investigation and geotechnics – diversity and sustainability. London: Society for Underwater Technology, pp. 341–356.

Randolph, M.F. (2004). Characterization of soft sediments for offshore applications. Geotechnical and Geophysical Site Characterization, Vol. 1 (Proc. ISC-2, Porto), Millpress, Rotterdam: 209-232.

Rix, G. J. & Stokoe K. H. II., (1991). Correlation of initial tangent modulus and cone penetration resistance. In Calibration chamber testing. New York: Elsevier, pp. 351–361.

Robertson, P.K., (1990). Soil classification using the cone penetration test. Canadian Geotechnical Journal, 27(1): 151-158.

Robertson, P.K., (2009). Interpretation of Cone Penetration Tests – a unified approach. Canadian Geotechnical Journal, 46: 1-19

Robertson, P.K., (2010). Evaluation of Flow Liquefaction and Liquefied strength using the Cone Penetration Test. Journal of Geotechnical and Geoenvironmental Engineering, ASCE, 136(6): 842-853

Robertson, P.K., (2015). Comparing CPT and Vs Liquefaction Triggering Methods. Journal of Geotechnical and Geoenvironmental Engineering, ASCE, 141(9): 842-853

Robertson, P.K., (2016), Cone penetration test (CPT)-based soil behaviour type (SBT) classification system: an update. Canadian Geotechnical Journal, 53(12); pp 1910-1927

Robertson. P.K., Campanella, R.G., Gillespie, D., and Greig, J., (1986). Use of Piezometer Cone data. In-Situ'86 Use of Ins-itu testing in Geotechnical Engineering, GSP 6, ASCE, Reston, VA, Specialty Publication, SM 92, pp 1263-1280.

Robertson, P.K. and Wride, C.E., (1998). Evaluating cyclic liquefaction potential using the cone penetration test. Canadian Geotechnical Journal, Ottawa, **35**(3): 442-459.

Robertson, P.K., Wride (Fear), C.E., List, B.R., Atukorala, U., Biggar, K.W., Byrne, P.M., Campanella, R.G., Cathro, D.C., Chan, D.H., Czajewski, K., Finn, W.D.L., Gu, W.H., Hammamji, Y., Hofmann, B.A., Howie, J.A., Hughes, J., Imrie, A.S., Konrad, J.-M., Küpper, A., Law, T., Lord, E.R.F., Monahan, P.A., Morgenstern, N.R., Phillips, R., Piché, R., Plewes, H.D., Scott, D., Sego, D.C., Sobkowicz, J., Stewart, R.A., Watts, B.D., Woeller, D.J., Youd, T.L., and Zavodni, Z. (2000). The CANLEX project: summary and conclusions. Canadian Geotechnical Journal, 37: 563–591.

Safner, D.A., Jung, Y., Hryciw, R.D. and Green, M., (2011), Comparison of predicted cyclic resistance ratios from CPT, DMT and shear wave velocity tests in Griffin, Indiana. Proceedings of Geo-Frontiers, ASCE, pp 2298-2307.

Saye, S. R., Santos, J., Olson, S.M. and Leigh, R.D. (2017). Linear trendlines to assess soil classification from cone penetration test data. J. Geotech. Geoenviron. Eng. 143(9): 04017060.

Schnaid, F. 2009. In-Situ Testing in Geomechanics – the main tests. Taylor & Francis Group, London: 327 p.

Schnaid, F. & Odebrecht, E. (2015) Challenges in the interpretation of the DMT in tailings. The 3rd Int. Conf. on the Flat Dilatometer DMT-15, Rome, 13-24.

Schneider, J.A., Randolph, M.F., Mayne, P.W. and Ramsey, N. R., (2008). Analysis of Factors Influencing Soil Classification using Normalized Piezocone Tip Resistance and Pore Pressure Parameters. Journal of Geotechnical and Geoenvironmental Engineering, ASCE, 134(11): 1569-1586.

Schneider, J.A. and Lehane, B.M., (2010). Evaluation of cone penetration testing from a calcareous sand dune. Proceedings International Symposium on Cone Penetration Testing, CPT'10, Huntington Beach, CA, paper 2-28, www.cpt10.com

Schneider, J.A. and Moss, R.E.S., (2011). Linking cyclic stress and cyclic strain based methods for assessment of cyclic liquefaction triggering in sands. Geotechnique Letters, Institute of Civil Engineers, UK

Schneider, J.A., Hotstream, J.N., Mayne, P.W. and Radolph, M.F., 2012, Comparing CPTU Q-F and Q-$\Delta u_2/\sigma'_{vo}$ soil classification charts. Geotechnique Letters 000, 1–7, http://dx.doi.org/10.1680/geolett.12.00044, 7 pages.

Simonini, P., (2004), Characterization of Venice lagoon silts from in-situ tests and performance of a test embankment. Proceedings 2nd International Conference on Site Characterization, ISC'2, Geotechnical & Geophysical Site Characterization, Porto, Vol. 1, 187-207.

Wride, C.E., Robertson, P.K., Biggar, K.W., Campanella, R.G., Hofmann, B.A., Hughes, J.M.O., Küpper, A., and Woeller, D.J. (2000) In-Situ testing program at the CANLEX test sites. Canadian Geotechnical Journal, Vol. 37, No. 3, June, pp. 505-529.

**Table 1: Selected representative examples**

| Ref # | Site | Description | Geologic Age | $Q_{tn}$ | $F_r$ | $U_2$ | $I_G$ | $K^*_G$ | References |
|---|---|---|---|---|---|---|---|---|---|
| 1 | San Francisco (USA) | Young Bay Mud NC-LOC Clay | Holocene | 4.0 (3.0-5.0) | 1.0 (0.5-2.0) | 2.0 (1.5-3.0) | 30 (25-35) | 85 (70-100) | Robertson (personal files) |
| 2 | Burswood Perth (Australia) | NC-LOC Clay | Holocene | 6.5 (5.5-8.0) | 2.0 (1.0-3.0) | 2.5 (1.5-3.5) | 22 (18-30) | 90 (75-122) | Randolph, 2004 |
| 3 | Syncrude (Canada) | NC Tailing Sand | Recent | 30 (20-65) | 0.7 (0.4-1.0) | 0 | 8 (6-10) | 105 (100-110) | Wride et al, 2000 |
| 4 | Highmont (Canada) | NC Tailing Sand | Recent | 40 (20-70) | 0.3 (0.1-0.6) | 0 | 8 (6-12) | 130 (120-140) | Wride et al, 2000 |
| 5 | LL Dam (Canada) | NC Tailing Sand | Recent | 45 (30-60) | 0.4 (0.1-0.8) | 0 | 8 (6-12) | 140 (130-150) | Wride et al, 2000 |
| 6 | Holmen (Norway) | Drammen River NC Sand | Holocene | 30 (20-60) | 0.4 (0.2-0.7) | 0 | 12 (10-18) | 155 (125-205) | Lunne et al., 2003 |
| 7 | Onsoy (Norway) | NC-LOC Clay | Holocene | 4.5 (4.0-5.0) | 1.8 (1.2-2.2) | 3.0 (2.5-3.5) | 60 (50-70) | 185 (155-215) | Lunne et al., 1997 |
| 8 | Tabarao (Brazil) | NC-LOC Clay | Holocene | 4.0 (3.0-5.0) | 1.3 (1.1-1.5) | 1.7 (1.0-2.2) | 65 (50-80) | 185 (140-225) | Schnaid et al., 2015 |
| 9 | UBC McD. (Canada) | Fraser River NC Sand | Holocene | 100 (50-150) | 0.3 (0.2-0.5) | 0 | 5 (3-9) | 200 (100-300) | Campanella et al, 1983 |
| 10 | KIDD (Canada) | Fraser River NC Sand | Holocene | 80 (40-150) | 0.6 (0.3-1.0) | 0.1 (-0.1-0.5) | 8 (5-12) | 214 (130-310) | Wride et al, 2000 |
| 11 | J-Pit (Canada) | NC Tailing Sand | Recent | 35 (20-50) | 0.7 (0.6-1.0) | 0 | 15 (9-25) | 215 (170-270) | Wride et al, 2000 |
| 12 | KIDD (Canada) | Fraser River NC-LOC Clay | Holocene | 3.5 (3.0-4.0) | 1.1 (0.9-1.4) | 3.0 (2.0-3.5) | 85 (60-110) | 215 (155-280) | Wride et al, 2000 |
| 13 | Bothkennar (UK) | LOC silty Clay | Holocene | 6.5 (5.5-8.0) | 1.6 (1.0-2.5) | 3.6 (2.5-4.5) | 60 (50-70) | 240 (205-290) | Hight et al, 2003 |
| 14 | UBC McD. (Canada) | Fraser River NC-LOC Clay | Holocene | 4.0 (3.0-5.0) | 1.8 (1.5-2.2) | 2.5 (2.0-3.0) | 100 (80-120) | 280 (230-320) | Campanella et al, 1983 |
| 15 | San Francisco (USA) | Old Bay Clay OC Clay | Late Pleistocene | 12.0 (5-30) | 2.5 (1.5-5.0) | 2.5 (-1.5-5.0) | 45 (30-100) | 300 (195-600) | Robertson (personal files) |
| 16 | Venice (Italy) | NC-LOC Clayey Silt | Holocene | 7.5 (5.0-10.0) | 2.0 (1.3-2.8) | 1.0 (0.1-1.8) | 70 (60-80) | 315 (270-350) | Simonini et al., 2004 |
| 17 | Amherst (USA) | Varved clay | Late Pleistocene | 7.5 (6.5-9.0) | 1.5 (0.8-3.0) | 5.0 (3.0-6.0) | 70 (50-90) | 325 (225-400) | DeGroot & Lutenegger, 2003 |
| 18 | Ford Center (USA) | LOC Clay | Pleistocene | 7 (5.5-9.0) | 3.0 (2.5-43.5) | 3.8 (3.0-4.5) | 78 (70-90) | 330 (300-380) | Finno et al 2000 |
| 19 | Madingley (UK) | HOC Clay | Cretaceous | 35 (30-45) | 4.5 (3.0-6.0) | -1 | 25 (15-30) | 360 (330-430) | Lunne et al, 1997 |
| 20 | Griffin (USA) | Dense Sand | Pleistocene | 150 (80-400) | 0.6 (0.3-1.0) | 0 | 9 (4-20) | 380 (215-800) | Safner et al, 2011 |
| 21 | Tangiers (Morocco) | Calcareous sand | Recent | 100 (60-200) | 0.2 (0.1-0.8) | 0 | 12 (7-20) | 380 (215-560) | Debats et al, 2015 |
| 22 | Campinas (Brazil) | Residual soil | - | 20 (15-25) | 6.0 (5.0-8.0) | 1 (0-4) | 45 (40-60) | 425 (375-565) | De Mio et al, 2010 |
| 23 | Dubai (UAE) | Calcareous sand | Recent | 70 (60-80) | 0.2 (0.1-0.3) | 0 | 18 (15-21) | 435 (360-500) | Robertson, (personal files) |
| 24 | Porto (Portugal) | Residual soil | - | 40 (30-50) | 5.0 (3.0-7.0) | 0 | 30 (20-40) | 475 (320-640) | De Mio et al, 2010 |
| 25 | Ledge Point (W. Australia) | Calcareous sand | Holocene | 150 (80-300) | 0.5 (0.2-0.8) | 0 | 10 (5-20) | 500 (330-800) | Schneider & Lehane, 2010 |
| 26 | Houston (USA) | Beaumont OC Clay | Pleistocene | 25 (20-30) | 4 (3.5-4.5) | -0.5 (-1.0 – 0) | 48 (35-50) | 535 (425-640) | Mayne, 2009 |
| 27 | Atlanta (USA) | Piedmont Residual soil | - | 45 (25-65) | 2.2 (1.2-3.0) | -0.5 (-1.0-0) | 33 (25-40) | 570 (470-640) | Mayne, 2009 |
| 28 | Charleston (USA) | Cooper Marl Calcareous Clay | Oligocene | 12 (8-25) | 0.6 (0.4-1.4) | 6 (4.5-11) | 90 (50-200) | 580 (330-1200) | Camp et al 2002 |
| 29 | Los Angeles (USA) | Fernando Siltstone | Miocene | 75 (60-100) | 1.5 (1.0-2.0) | 33 (20-40) | 30 (17-40) | 635 (510-1,020) | Robertson, (personal files) |
| 30 | Anchorage (USA) | Bootlegger Cove HOC Clay | Pleistocene | 20 (10-50) | 1.3 (1.0-2.0) | 1.7 (1.0-5.5) | 80 (50-110) | 750 (450-1,400) | Mayne & Pearce, 2005 |
| 31 | Windsor (USA) | Calcareous cemented clay | Miocene | 45 (40-50) | 2.5 (2.0-3.0) | 12 (5-16) | 48 (40-65) | 830 (690-1,150) | Ku et al, 2013 |
| 32 | Calgary (Canada) | Glacial clay Till | Pleistocene | 40 (35-50) | 3.0 (2.5-3.5) | 5 (0-7.0) | 55 (40-70) | 850 (600-1,100) | Mayne & Woeller, 2008 |
| 33 | Newport Beach (USA) | Monterey Sandstone/siltstone | Miocene | 150 (50-400) | 2.5 (0.8-5.0) | 1 (0-15) | 20 (8-200) | 860 (350-4,000) | Bastani et al, 2014 |

*Values shown are mean values with range in bracket*
*NC Normally consolidated*
*LOC Lightly overconsolidated (OCR < 4)*
*HOC Heavily overconsolidated (OCR >4)*

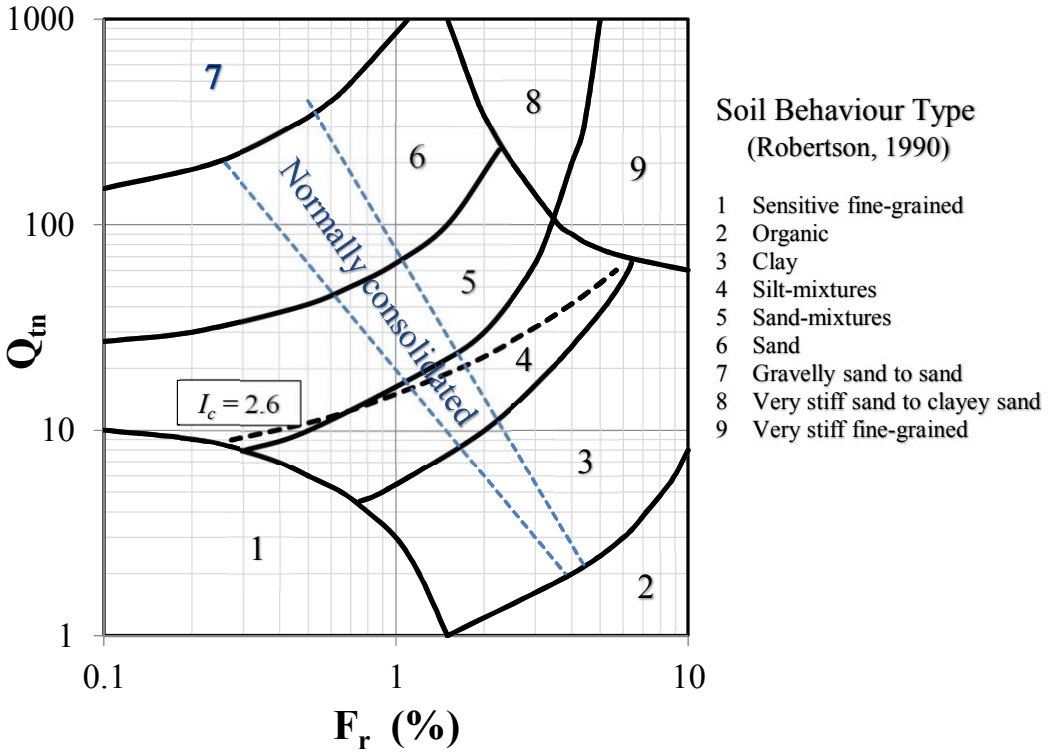


**Figure 1: CPT-based SBTn chart suggested by Robertson (1990) and updated by Robertson (2009)**

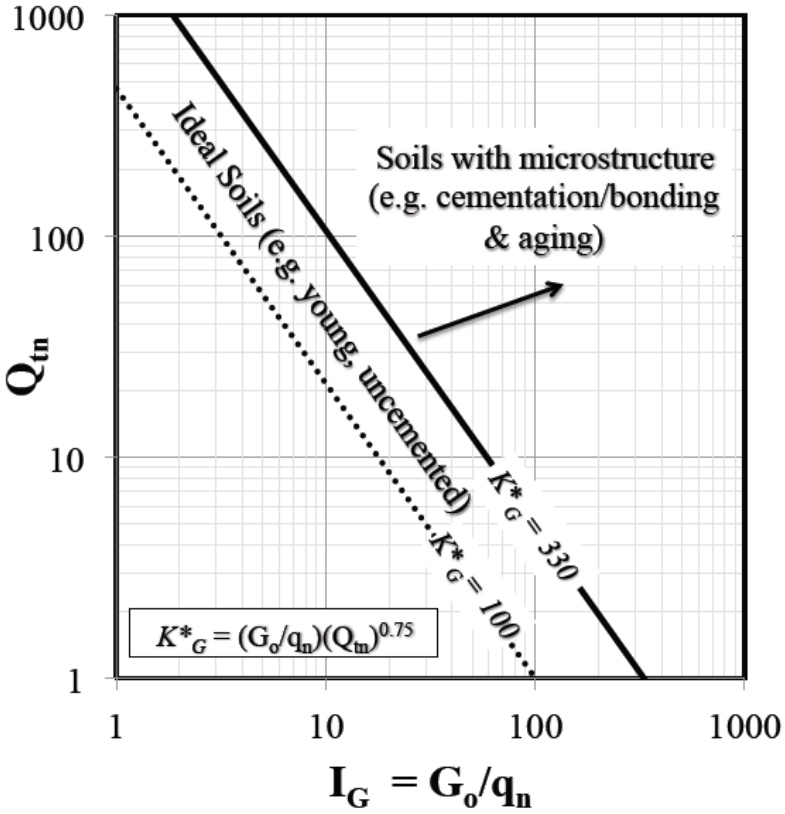


**Figure 2: Proposed $Q_{tn}$ – $I_G$ chart to identify soils with microstructure**

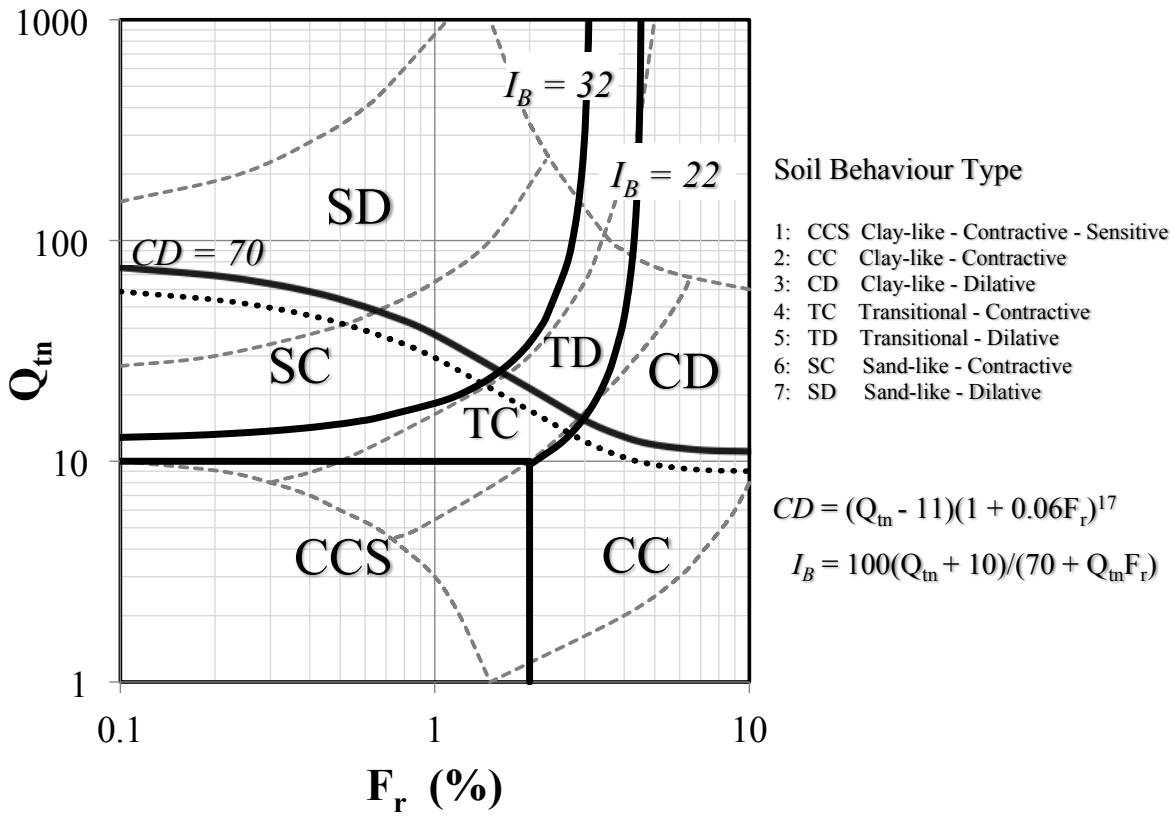


**Figure 3: Proposed updated SBTn chart based on $Q_{tn} – F_r$ (solid lines show proposed new soil behavior type boundaries and dashed lines show boundaries suggested by Robertson, 1990)**

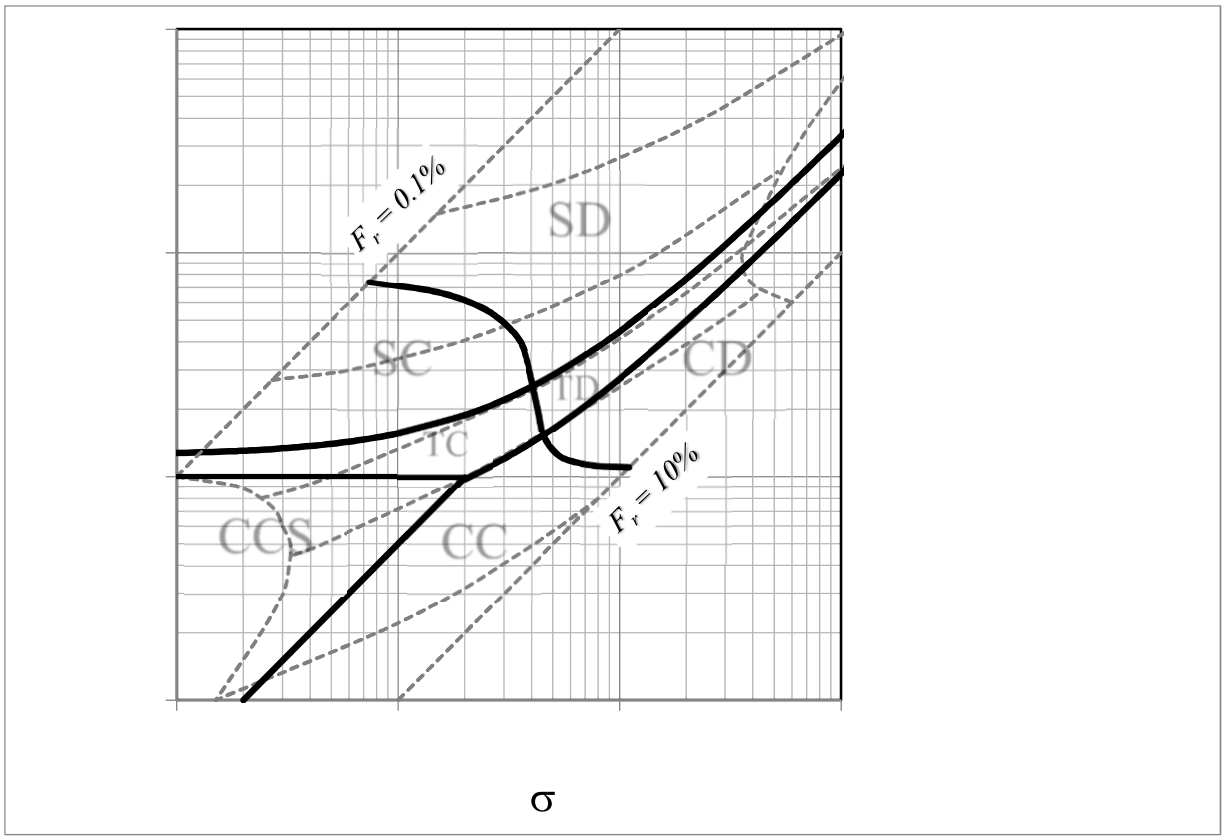


**Figure 4: Proposed alternate format SBTn chart based on $Q_{tn}$ – F (solid lines show proposed new soil behavior type boundaries and dashed lines show boundaries suggested by Robertson, 1990)**

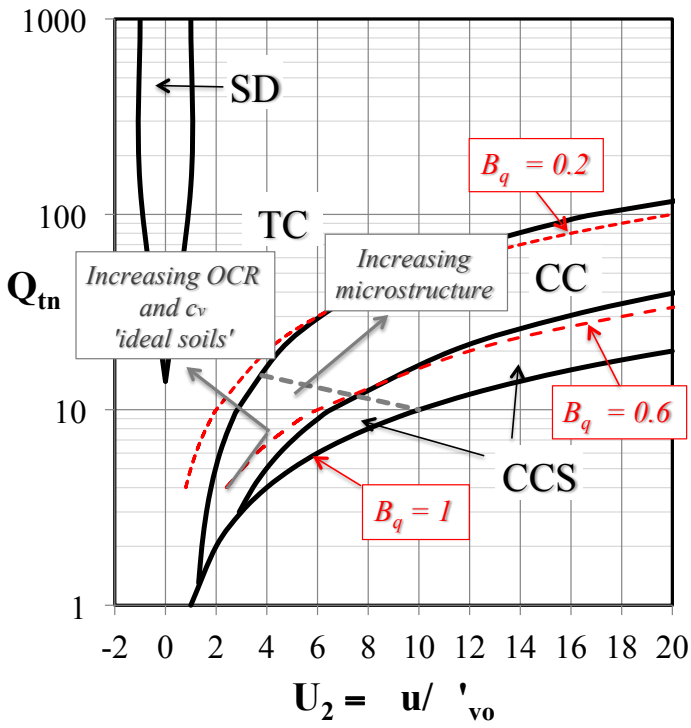


**Figure 5: Proposed updated Schnieder et al (2008) chart based on $Q_{tn}$ – $U_2$ with proposed new soil behavior type boundaries ($B_q$ lines in red)**

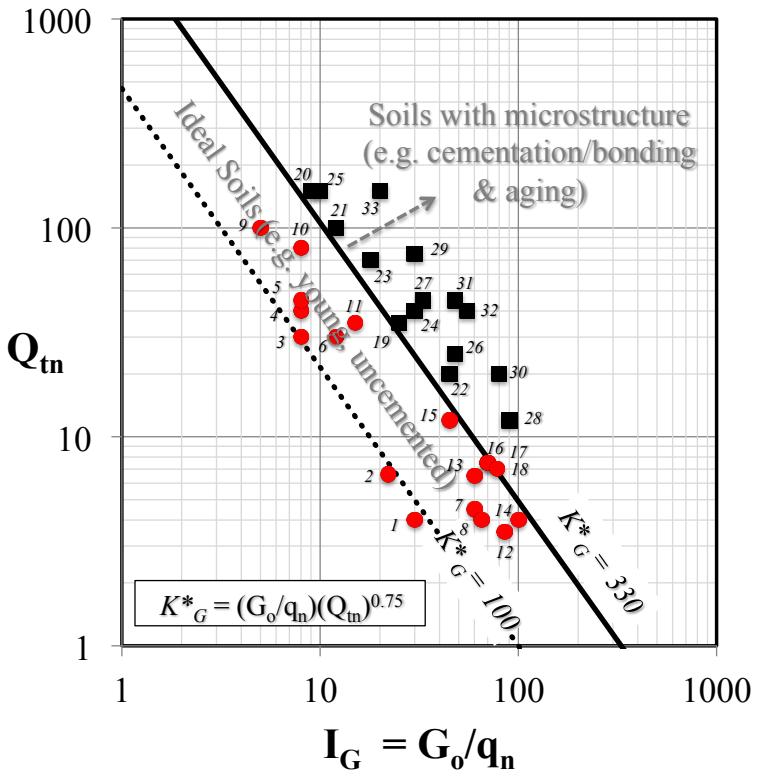


**Figure 6: Proposed $Q_{tn}$ – $I_G$ chart with case history examples (details in Table 1). Red circles are young uncemented, and Black squares are soils with microstructure or calcareous.**

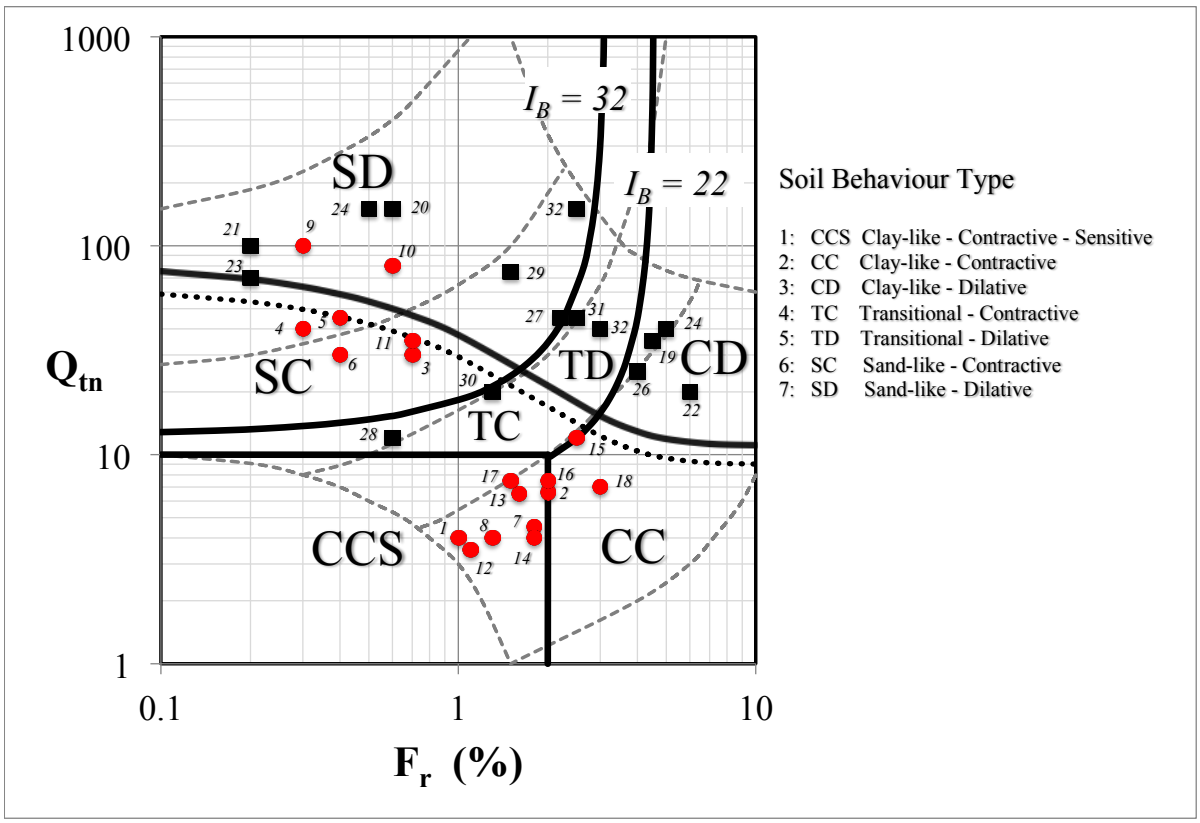


**Figure 7: Proposed updated SBTn chart based on $Q_{tn} - F_r$ with case history examples (details in Table 1). Red circles are young uncemented; and Black squares are soils with microstructure or calcareous.**

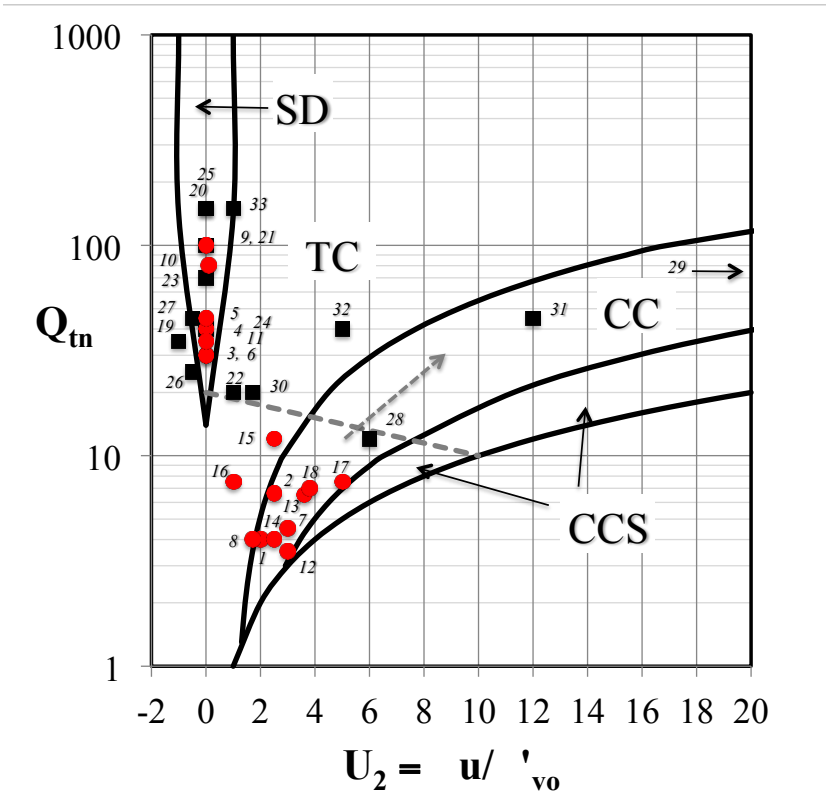


**Figure 8: Proposed updated Schnieder et al (2008) chart based on $Q_{tn} - U_2$ with case history examples (details in Table 1. Red circles are young uncemented, Black squares are soils with microstructure or calcareous)**

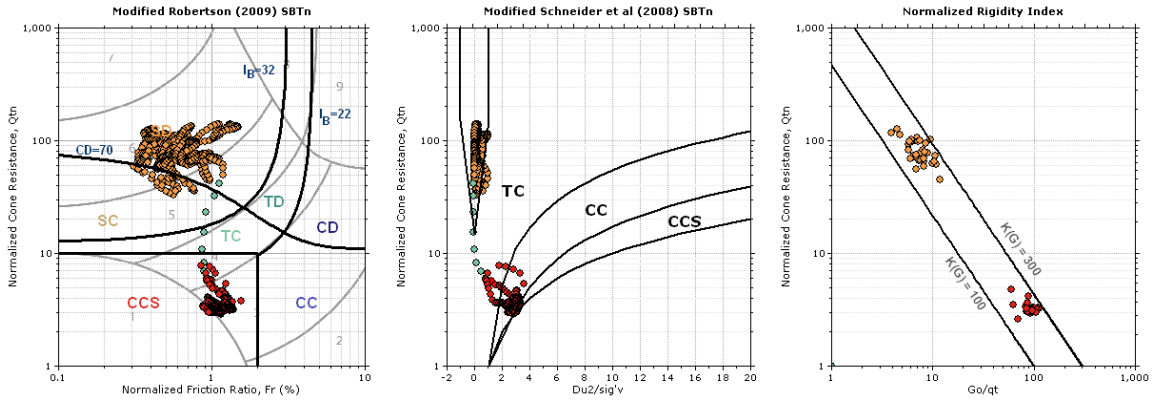


**Figure 9: Example of normalized SCPTu data from 4m to 40m at the KIDD site in the Fraser River delta near Vancouver, BC, (orange dots for the sand from 4m to 22.7m, red dots for clay from 22.9 to 40m, green dots for the transition zone from 22.7 to 22.9m)**

(a)

(b)

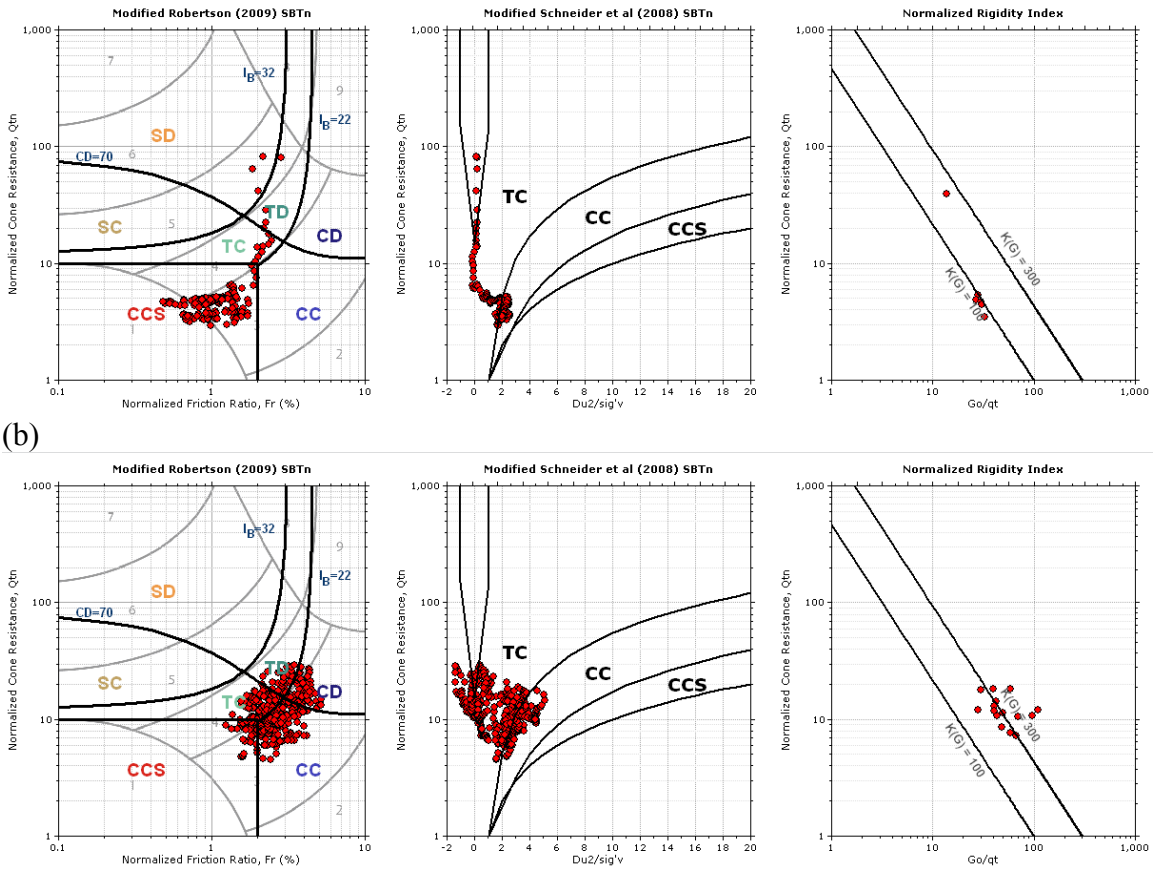


**Figure 10: Example normalized SCPTu data from San Francisco Bay, California, USA; (a) Young Bay Mud with desiccated crust (2m to 11m) and (b) Old Bay Clay (12 to 35m)**

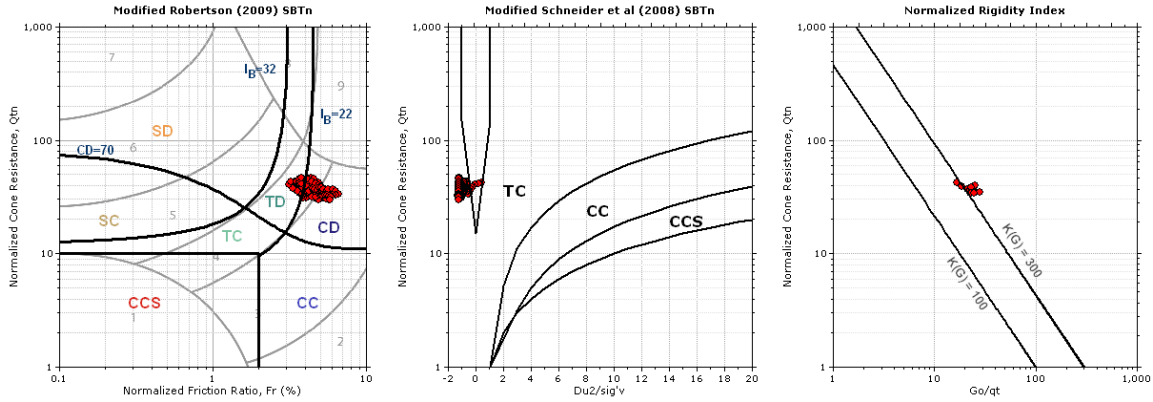


**Figure 11: Example normalized SCPTu data from 2m to 12m at the Madingley stiff clay site, Cambridge, UK**

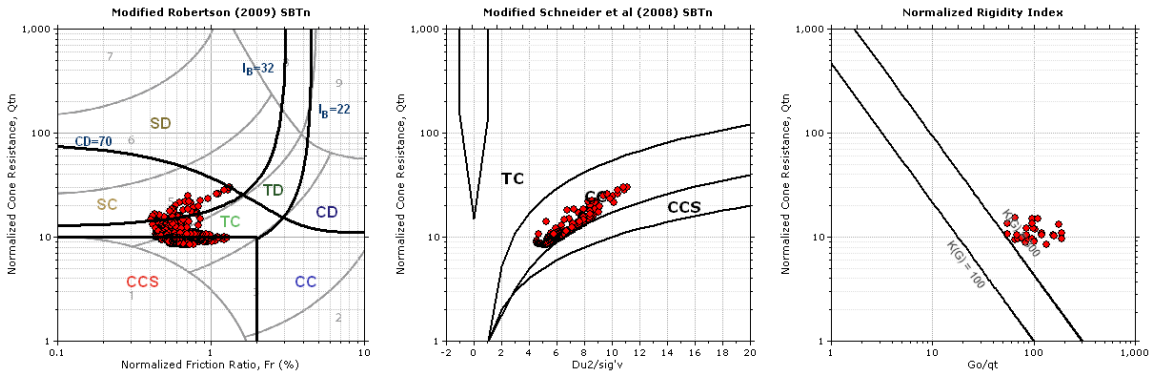


**Figure 12: Example normalized SCPTu data from 22m to 50m in Cooper Marl (calcareous cemented clay), Charleston, South Carolina, USA**

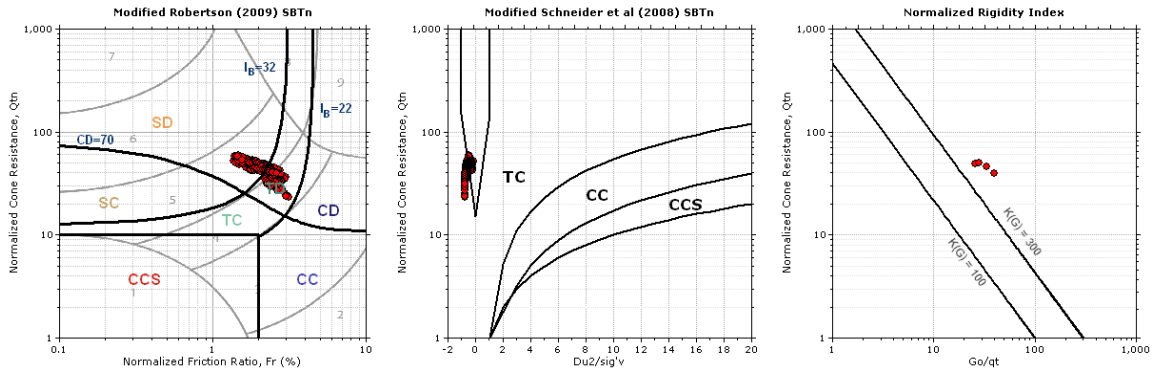


**Figure 13: Example normalized SCPTu data from 4m to 19m in Piedmont residual soil at a site in Atlanta, Georgia**

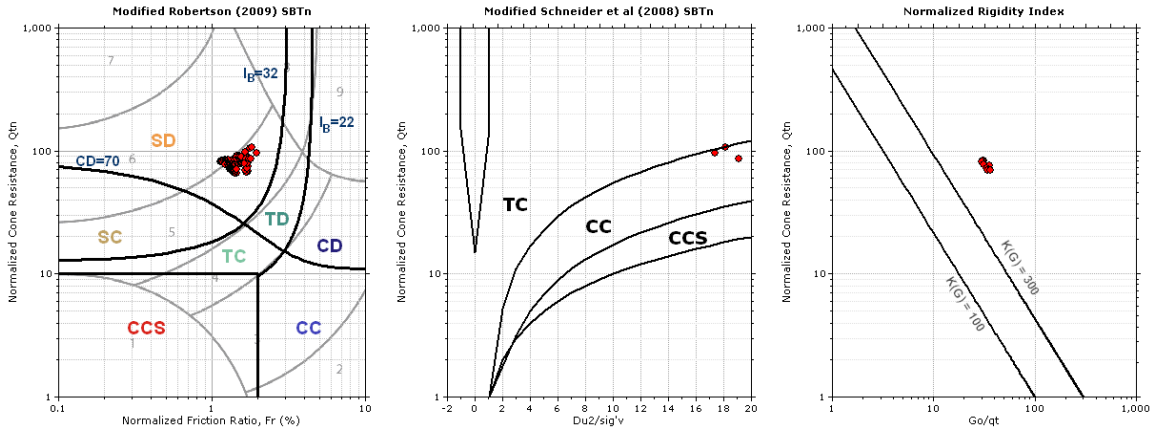


**Figure 14: Example normalized SCPTu data from 3m to 10m in siltstone at a downtown Los Angeles site, California**

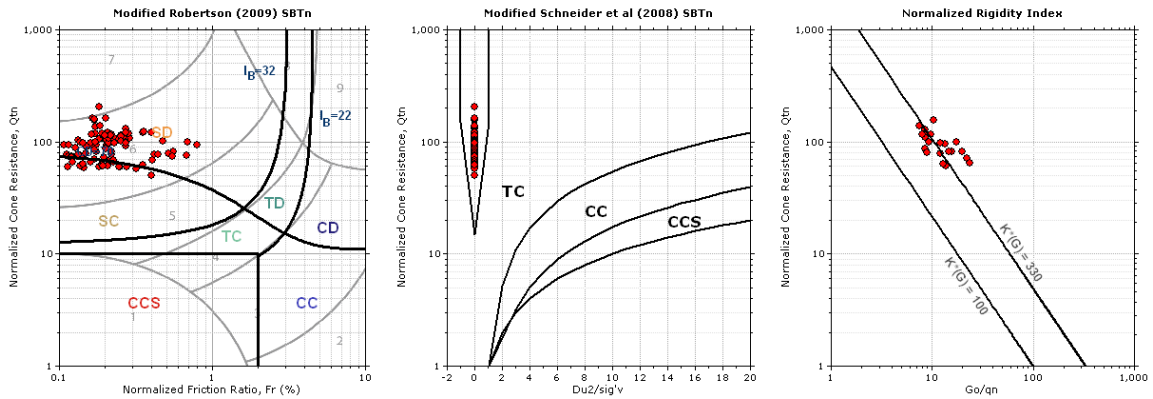


**Figure 15: Example normalized SCPT data from 4m to 14m in hydraulically placed calcareous sand in Tangier, Morocco (data from Debats et al, 2015)**